AD-A071 286 MASSACHUSETTS INST OF TECH CAMBRIDGE DEPT OF OCEAN E--ETC F/G 13/10
ANALYSIS OF THE LATERAL FORCE COEFFICIENT FOR SHIP MANEUVERING --ETC(U)
JUN 76 R STANLEY N00014-75-C-1006

UNCLASSIFIED NL

| OF 2

AD
A071286

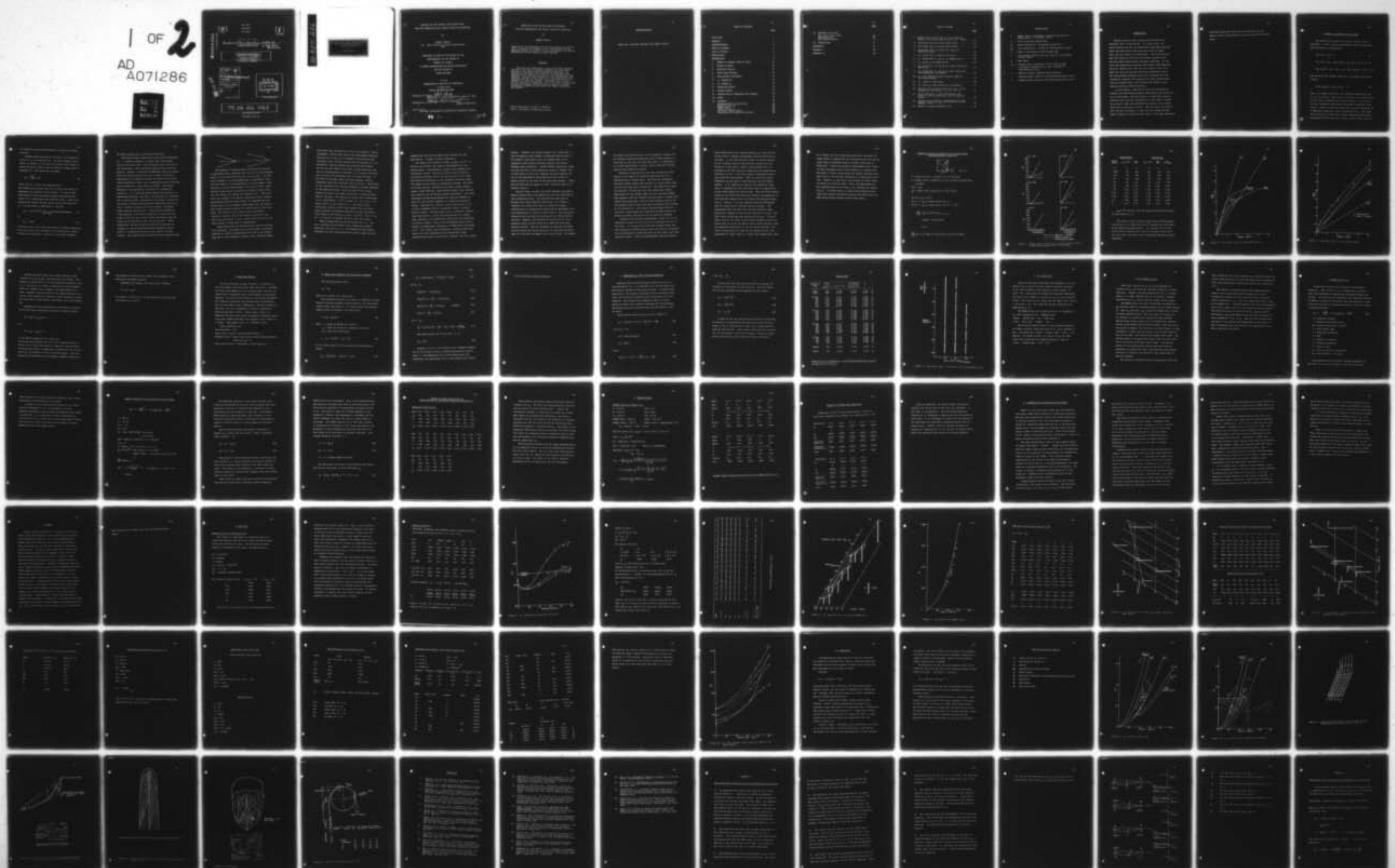

AD A071286

DDC ACCESSION NUMBER

II

LEVEL

DATA SHEET

PHOTOGRAPH

THIS SHEET

1

INVENTORY

Analysis of the Lateral Force Coefficient------

DOCUMENT IDENTIFICATION

by Robt. Stanley
Dtd. June '76

DISTRIBUTION STATEMENT A
Approved for public release;
Distribution Unlimited

DISTRIBUTION STATEMENT

Accession For	
NTIS GRA&I	☒
DDC TAB	☐
Unannounced	☐
Justification	
Per FL-88 (R77-2446) (2nd Request)	
By on file	
Distribution/	
Availability Codes	
Dist	Avail and/or special
A	

DDC FILE COPY

DISTRIBUTION STAMP

DDC
RECEIVED
JUL 17 1979
D

DATE ACCESSIONED

79 06 26 063

DATE RECEIVED IN DDC

PHOTOGRAPH THIS COPY

ANALYSIS OF THE LATERAL FORCE COEFFICIENT FOR SHIP MANEUVERING AND DYNAMIC STABILITY EQUATIONS

by

ROBERT STANLEY
B.S. Webb Institute of Naval Architecture
1970

SUBMITTED IN PARTIAL FULFILLMENT OF THE
REQUIREMENTS FOR THE DEGREE OF
MASTER OF SCIENCE
IN NAVAL ARCHITECTURE AND MARINE ENGINEERING
AND THE DEGREE OF
OCEAN ENGINEER

at the

MASSACHUSETTS INSTITUTE OF TECHNOLOGY

22 June 1976

Contract No N00014-75-C-1006

Signature of Author. Robert Stanley . . . .
Department of Ocean Engineering, June 22, 1976

Accepted by. Martin A. Abkowitz . . . .
Thesis Supervisor

Certified by . . . .
Chairman, Departmental Committee on Graduate Students

79 06 26 065

062-512
JUN 19 1978

ANALYSIS OF THE LATERAL FORCE COEFFICIENT

FOR SHIP MANEUVERING AND DYNAMIC STABILITY EQUATIONS

by

ROBERT STANLEY

Submitted to the Department of Ocean Engineering on June 22, 1976, in partial fulfillment of the requirements for the degree of Master of Science in Naval Architecture and Marine Engineering and the degree of Ocean Engineer.

ABSTRACT

The hull lift coefficient is one of the most important and one of the least tractable components of the dynamic straight-line stability and maneuvering equations. An analysis of the basic flow condition has been made, and similarities to theories and data for flat plates have been examined. The hull flow condition is too complicated to be compared directly to flat plate flow conditions, but useful insight still has been gained. Available data for wing sections and sets of systematic hull series have shown trends of lift coefficient versus B/L and C_B, and have allowed rudimentary analyses of the effects of skegs, propellers, and rudders.

Thesis Supervisor: Martin A. Abkowitz

Title: Professor of Ocean Engineering

ACKNOWLEDGEMENT

Thank you, Professor Abkowitz and Debbie Schmitt.

TABLE OF CONTENTS

Page

LIST OF FIGURES

NOMENCLATURE

A - aspect ratio = span^2/area [treating ship hull as a double body, $A = (2T)^2/2TL = 2T/L$]

B - ship or section maximum beam

C_B - block coefficient = displaced volume/$L \cdot B \cdot T$

C_L - lift coefficient = lift/$\frac{1}{2}\rho U^2$ (characteristic area)

D - drag or resistance of water-borne body

L - ship length, usually Lbp, but also Lwl for purposes of this report

T - ship draft

Y_v - lateral force coefficient on hull due to sway
$= -$(Lift/$\frac{1}{2}\rho U$ characteristic area + Drag/$\frac{1}{2}\rho U^2$ characteristic area)

α - angle of attack, measured from centerline

$'$ - (single prime) refers to non-dimensionalization by L^2

$''$ - (double prime) refers to non-dimensionalization by LT

INTRODUCTION

Dynamic stability and turning characteristics are important items in ship design. In recent years, the course-keeping problems of supertankers have made headlines which have made naval architects more aware of rudder, skeg, and hull design for maneuvering. Less heralded have been the studies of turning that warship, patrol craft, and high speed containership designers have made. In the first two categories, designers have sought "high maneuverability," meaning that they want the ships to "turn on a dime" yet still go straight ahead when directed to do so. The containership designers have been concerned with the "excessive" straight line stability of their high-powered, long and slender ships, since getting the ships to turn requires enormous control surfaces.

In this report, I had set out with the intention of studying the maneuvering problem, specifically the derivative Y_v, of high speed, long and slender, transom stern vessels. Although some very nice photographs of flow under a transom stern patrol craft were published by Saunders, very little quantitative data was available. The net result, in dealing with the data available, is that much more study has been made of medium to very full hull forms. A few data points for

individual destroyer-type ships are plotted, but the general trends and analyses are derived from the full-form ships.

1. THEORY OF LATERAL FORCE ON SHIPS

The generalized equations of motion, as set forth in Reference 2, yield a linear mathematical model for steering and maneuvering a surface ship:

$$(X_{\dot{u}} - m)\dot{u} + X_u \Delta u = 0 \tag{1}$$

$$(Y_{\dot{v}} - m)\dot{v} + Y_v v + (Y_{\dot{r}} - mx_G)\dot{r} + (Y_r - mu_1)r + Y_\delta \delta = 0 \tag{2}$$

$$(N_{\dot{v}} - mx_G)\dot{v} + N_v v + (N_{\dot{r}} - I_z)\dot{r} + (N_r - mx_G u_1)r + N_\delta \delta = 0 \tag{3}$$

The criterion for dynamic stability in straight line motion follows:

$$Y_v(N_r - mx_G u_1) - N_v(Y_r - mu_1) > 0 \tag{4}$$

Thus, for dynamic stability, the important coefficients are Y_v, Y_r, N_v, and N_r. The first, Y_v = lateral force coefficient, is not easy to calculate by analytic methods. It is one of the most important coefficients and requires accuracy to be useful. Jacobs [17,18] has shown that N_v can be estimated as a subsequent operation to the calculation of Y_v. The value for Y_r usually is quite small, hence simplified calculation procedures suffice. The value for N_r, though large, also can

be treated by simplified procedures to obtain sufficient accuracy.

Attempts have been made in the past to fit empirical curves for Y_v to existing data. The most commonly cited effort is Jacobs' [17,18] use of the Jones [19] formula to treat bare hulls, then to add the effect of large area of deadwood aft. The result was a formula:

$$Y_v'' = \frac{\partial C_L''}{\partial \alpha} + D_o'' \tag{5}$$

where $\partial C_L''/\partial\alpha = \pi A$ for the complete ship.
The formula gives values that are "of the right orders of magnitude and indicate correct trends." It can be seen from Figure 11 that the formula always overpredicts the value of Y_v' even without the addition of D_o'. Inoue [16] modified the Jacobs formula, making use of the fact that D_o' is quite small in comparison to $\partial C_L'/\partial\alpha$:

$$Y_v' = 1.6\pi\,(T^2/L^2) \text{ plus a correction multiplier for trim} \tag{6}$$

or

$$Y_v'' = .8\,\pi A \tag{7}$$

Gerritsma et.al. [12] cited this formula as being principally based on Bollay's [6] low aspect ratio theory and a number of empirical allowances. However, it very much resembles

the Jones formula with a correction multiplier.

The Jones formula indeed does a fair job of predicting Y_v'. It takes no account of factors other than aspect ratio of the basic hull. This objection alone certainly is not significant, since correction factors easily could be applied. However, a much more fundamental objection exists. The Jones formula was derived from a sound, theoretical examination of triangular or delta low aspect ratio wings. Jones considered a long, flat, triangular airfoil travelling point-foremost at a small angle of attack. The theory depended on the expansion of sections in a downstream direction. It is true that ships expand from the bow in a downstream direction, but this is an expansion in thickness, not in section width. According to the theory, any part of the airfoil surface having parallel sides would develop no lift. Further, sections aft of the section of maximum width would not develop lift. Jones used an assumption, "corresponding to the Kutta condition," to show that the shape of the foil aft of the section of maximum width has little or no influence on the lift of the foil. Jones showed that the tip of the foil need not be pointed; an elliptic or similar plan-form having expanding section-width in a downstream direction gives nearly the same results. The reason can be surmised from the figures below:

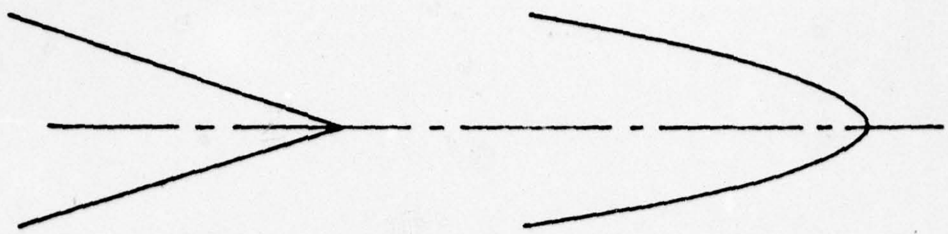

The evidence of observations of flow over the bottom of ship model hulls indicates that the lift on ships depends heavily on the conditions near the trailing edge. An ideal fluid treatment of a wing-shaped body in unbounded, inviscid flow results in the generation of a large moment, often referred to as the "Munk moment" [21], but no lift. Examination of the result of including viscosity reveals that net lift forces are created (see Appendix II). "The total lift, as a result of an inertia distribution and a viscous distribution along the ship length, is generated for the greater part in the forebody, which means that the viscous part counter-balances nearly the inertia part in the afterbody. The center of the viscous force distribution therefore lies well aft of the center of gravity." [12] This last point makes it quite evident that the fit of the Jones formula to ship data is happenstance.

Jones stated that the theory was not good for rectangular planforms. He showed that for such forms, the theory predicts an infinite concentration of lift at the leading edge and no lift elsewhere, whereas a more accurate theory

would show some distribution of the lift rearward. Bollay introduced a theory that could treat rectangular planforms. Starting with a thin flat rectangular plate having very low aspect ratio, Bollay treated the lift problem as a 2-D phenomenon, ignoring leading and trailing edge effects. For the infinite aspect ratio case, Bollay found that the wing is hydrodynamically equivalent to a constant distribution of bound vortices whose axes lie along the span. At the ends of the span, these vortices separate, flowing downstream along the resultant velocity vector. Inclination of the vortices to the wing was assumed to be most important at the separation point, since the part of the vortex nearest the wing is the most influential in inducing downwash at the wing. The theoretical normal force coefficient is $C_N = N/\frac{1}{2}\rho U^2 \text{area} = 2\sin^2\alpha$; hence, at $\alpha = 0$, $C_N = 0$. For aspect ratios in the range $0 < A < 1$, the normal force coefficient retains a $\sin^2\alpha$ form, except that the slope $\partial C_N/\partial\alpha_o$ becomes increasingly positive, so that the coefficient takes on the form $C_N = C_1 \sin\alpha + C_2 \sin^2\alpha$. At $A = 1$, C_N vs. α is nearly a straight line up to the stall angle.

Bollay stated that the theory worked for $A = 0$ and $A = \infty$, and that the low aspect ratio formulation worked relatively well for $0 < A < 1$. The reasons for the gradual breakdown are that three-dimensional effects occur and that

leading edge and trailing edge effects change the lift distribution. Figures 13 and 15 show this.

The aspect ratio range for ships is about $.05 < A < .2$, which is well within the range of applicability of the Bollay theory. Unfortunately, ships do not resemble flat rectangular plates. The fore portions usually do have a rectangular planform, while the sterns often are cut away. The important difference is the thickness variation along the length and the shape of transverse sections. By virtue of several factors, including blunt bows, widely varying sterns, beamy sections, large Reynolds number flow, and bow wave effects, the end effects become significant. Even flat rectangular plates being operated at the free surface in water are not directly amenable to treatment by Bollay's theory. Bertrand [3], testing a small plate with $A = .26$, in fully submerged flow in a propeller tunnel, verified Bollay's theory. But Gerritsma, et.al., testing a 3-meters long plate with $A = .114$ at the free surface in a towing tank, obtained a lift coefficient about half that predicted by Bollay's theory. Part of the discrepancy may be attributable to measurement inaccuracy, as admitted by Gerritsma, et.al. More likely, the differences in testing conditions account for very different vortex and boundary layer characteristics due to cavitation, aeration, and free surface

effects. Crabtree, as cited by Jacobs [17], noted that a flat rectangular plate showed a pronounced suction peak in the pressure distribution near the leading edge, with a consequent steep adverse pressure gradient and laminar boundary layer separation. Jacobs further noted that "since the size and form of the separation region or 'bubble' has a large effect on the lift, Tsakonas cautioned against the use of the experimental measurements on flat plates to predict forces in the case of the ship-wing analogy." (This caution would seem to apply to Jones' theory as well as to Bollay's theory.)

The net result is that flat plate theories and experimental results have to be modified to suit the realities of flow around ship hulls. The bow and stern sections of merchant ship hulls (Mariner, Series 60, etc.) begin to resemble flat plates with sharp or squared-off edges. Transom-stern or cutaway-stern ships such as destroyers have less resemblance to plates at their sterns. The differences between plates and ship hull mid-bodies are another matter entirely. However, such differences should not be interpreted as being of such nature as to make the flat plate theories useless. What is necessary is some way to bridge the gap between the plates and hulls; to show how the hulls make not very good low aspect ratio, thick wings. To dismiss

the flat plate data entirely, to use instead a formula with an entirely unrelated theoretical origin simply because it runs close to the data for some ship hulls, is undesirable. It is more satisfactory to start from an idealized concept, then to work toward the reality.

Bertrand's study hints at why flat rectangular plate theory is not useful for directly predicting the lift characteristics of ship hulls. His data for rectangular and delta plates showed some decrease in C_L when sharp leading and side edges were rounded off. The shed-vortex sheet was observed to break away from the bottom edge further downstream for the rounded edges than for the sharp edges. This suggests that the rounding off more easily allowed flow around the bottom edge, from the high pressure side to the low pressure side, without the need to generate tip vortices at the forward end. This effect would be magnified by a ship hull, since bilges are round and the width across the bottom increases from the bow to the parallel mid-body.

Saunders [22] presented photographs (Figure 15) of the underwater portions of ship hulls to illustrate the flow at the shell. It is easy to see that the rounded bilges and wide expanses of bottom plating cause the flow to be anything but two-dimensional across the span (in this case, from free surface to keel). There is considerable cross flow being

swept downstream by the forward velocity, so that the flow on each side is changed considerably from the waterline to the keel. In the fore portions, there is little evidence of the trailing vortices that would be formed along the bottom of a flat plate. Hence, little viscous lift is produced by the fore portions (supporting the assertion by Gerritsma, et.al.). The stern skegs or deadwood present a very different flow problem. They are like flat plates themselves and do much to help generate trailing vortex systems. It is tempting to observe that skegs and large areas of deadwood aft look like good cases for application of the Jones formula for delta wings. They are delta shapes, fitted to the hulls with the hulls acting as groundboards so that effective aspect ratios are double the measured aspect ratios. However, it is not apparent from the photographs that the skegs act as isolated lifting surfaces. The photographs show that when the flow has reached a skeg, substantial changes in free-stream flow have occurred. The shed vortex system has been started by the keel. On hard chine vessels, the chine itself can be expected to act as a bottom edge on a very low aspect ratio lifting surface, with the consequent generation of its own vortex systems. The Jones formula may be of some use for predicting the lift generated by a small skeg on a large, full-bodied ship, such

as a tanker, but the interactions with hull flow make the Jones formula inappropriate for calculating the lift due to large skegs or deadwood areas on slender ships such as destroyers. [Note that Saunders' photographs are of ships in fully developed turns, being tested on a rotating arm. The angle of attack varies along the length, starting from about zero at the bow and increasing in a downstream direction. However, Y_v and $\partial C_L/\partial\alpha$ are defined for small angles of attack for the whole ship. Thus, the photographs are not representative of the flow at the forebody for generating Y_v. A uniform angle of attack should generate more cross flow forward and should generate the beginnings of a shed vortex system further forward than shown.]

2. RESULTS OF BOLLAY'S THEORY FOR LOW ASPECT RATIO FLAT RECTANGULAR PLATES [6]

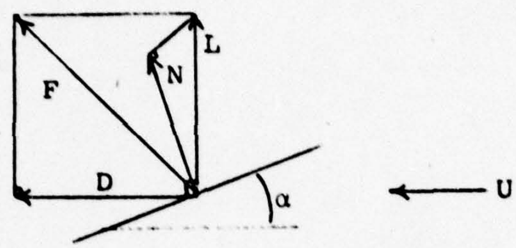

F = force on plate, resultant of lift and drag

N = normal force, component of lift resolved perpendicular to plate

$N/L = \cos\alpha$

C_N = normal force coefficient = $N/\frac{1}{2}\rho U^2$area

At $A = 0$, $C_N = 2\sin^2\alpha$

At $A = .5$, C_N is nearly linear with α

At $A = 1.$, C_N is linear with α for $0° < \alpha < 20°$

$$\frac{\partial C_L}{\partial \alpha_o} = \frac{\partial}{\partial \alpha}(2\sin^2\alpha/\cos\alpha)_{\alpha = 0,\ A = 0}$$

$$= 4\sin\alpha + 2\sin^3\alpha/\cos^2\alpha$$

$$= 0.0$$

$\frac{\partial C_L}{\partial \alpha_o}$ for $A > 0$ takes on increasingly positive values.

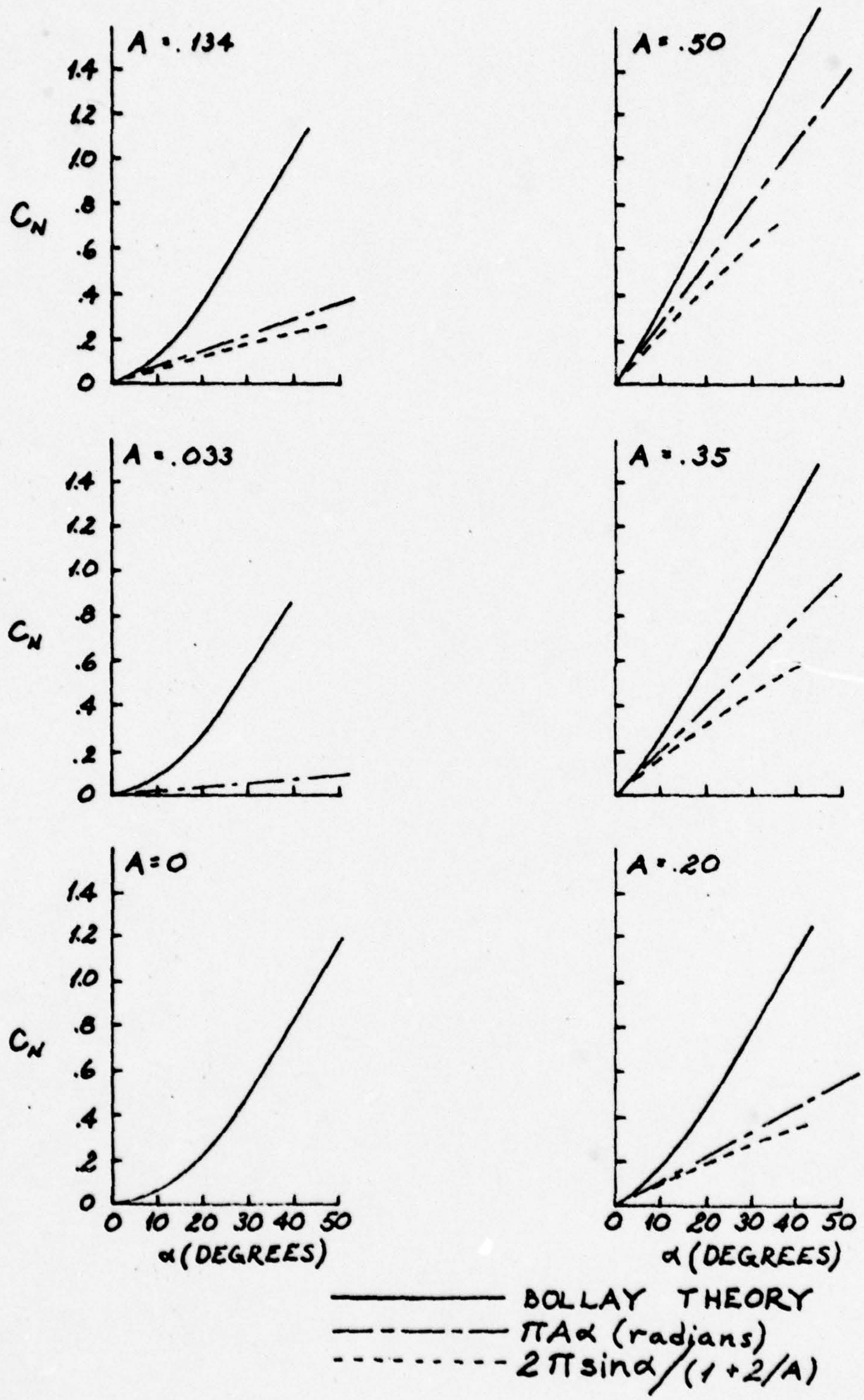

Figure 1: Normal Force Coefficient C_N versus Angle of Attack α for Various Aspect Ratio Flat Plates

	EXPERIMENTAL		THEORETICAL		
Aspect Ratio	C_N @ 30°	$\frac{\partial C_L}{\partial \alpha}$	C_N @ 25°	$\frac{\partial C_L}{\partial \alpha}$	$\frac{2\pi}{1 + 2/A}$
0	0	0	0	0	0
.0333	.14	.267	.08	.183	.103
.134	.34	.649	.20	.458	.393
.20	.42	.802	.33	.756	.571
.35	.62	1.18	.48	1.10	.936
.50	.90	1.72	.72	1.65	1.257
.66	1.05	2.01	1.00	2.29	1.559
1.00	1.33	2.54	1.28	2.93	2.094
1.25	1.40	2.67	1.55	3.55	2.417
1.5	1.50	2.86	1.60	3.67	2.693
2.	1.67	3.19	1.65	3.78	3.142

C_N at 30° and C_N at 25° are measured from lines tangent to the curves at $\alpha = 0$.

The plots of $\partial C_L/\partial\alpha$ versus A have been non-dimensionalized on $\frac{1}{2}\rho\,U\,L\cdot T$ rather than $\frac{1}{2}\rho\,U\,L^2$ because the first shows up the differences much better. The formulae of the form (coefficient x aspect ratio) plot as straight lines, while the non-linear low aspect ratio and Bollay theories are well separated.

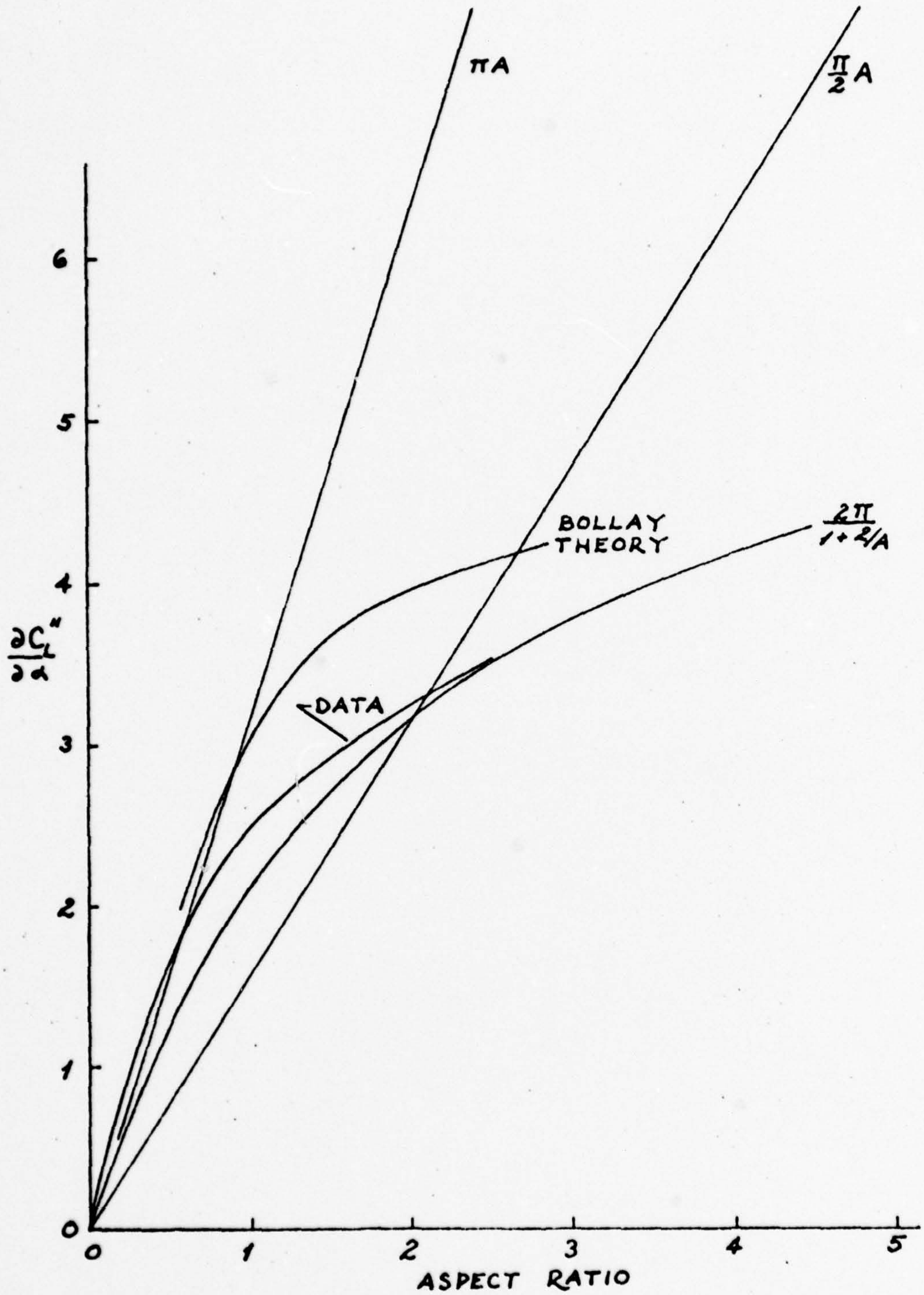

Figure 2: Lift-Slope $\partial C_L"/\partial\alpha$ versus Aspect Ratio

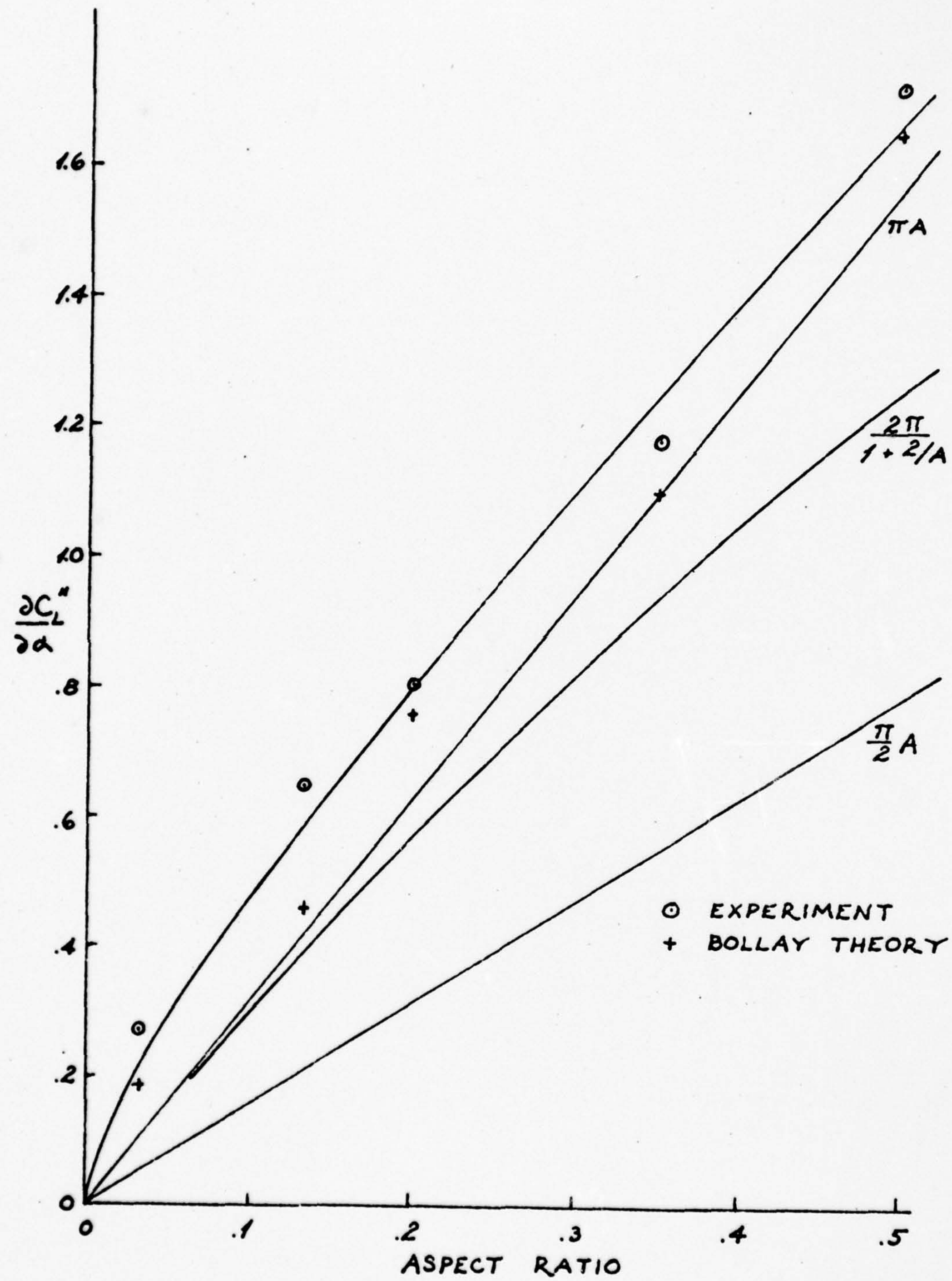

Figure 3: Lift-Slope $\partial C_L''/\partial\alpha$ versus Aspect Ratio

Within the ship aspect ratio range, Bollay's plots (Figure 1) of C_N versus α are distinctly non-linear. This causes no problem with Y_v' for the stability equation, since $Y_v' = (\partial C_L'/\partial\alpha_o) + D_o'$ which is defined for small perturbations in α about $\alpha = 0$, in Phase 1 and early Phase 2 of a turn. However, the non-linearity will affect the use of Y_v' in the linear maneuvering equation, where substantial values of α are used in later Phase 2 and Phase 3 of a turn (Figure 16).

Depending on the preferences of the authors, versions of the non-linear maneuvering equation include the terms

$$\Delta Y = Y_v v + Y_{v|v|} v|v| + \ldots$$

or

$$\Delta Y = Y_v v + Y_{vvv} v^3 + \ldots$$

in the Taylor expansions for forces [4].
The Bollay data indicate that the first expression gives a better fit to flat plate results. However, a lack of data for ship hulls makes it impossible to choose one form or the other for the purpose of fitting the data better. The non-linearities introduced by hull geometry probably complicate

the problem so much that any higher order between 2 and 3 would give acceptable results.

Landweber and Johnson [20] also cited a formula,

$$L = C_1\alpha + C_2\alpha^2$$

for bodies of revolution, but the exponent could have been 3 as easily as it was 2.

3. WING-SHIP ANALOGY

For the wing-ship analogy, the hull is treated as a very low aspect ratio fin having very large area. Although the hull's performance as a fin is quite poor, the area is large; hence, force/unit area x area becomes a significant quantity. As with all wing theories, the primary parameter for evaluating different lift coefficients for different hulls is the aspect ratio, span^2/area. The free surface of the water acts as a groundboard or mirror, effectively doubling the span's effect. Hence, span = draft x 2. Assuming that hulls have nearly rectangular planform, especially when rudders and skegs are included, area = draft x 2 x length. Then aspect ratio = $A = 4T^2/2TL = 2T/L$.

Other parameters are:

thickness/chord = B/L

taper ratio = C_t/C_s = tip chord/root chord ≈ 1

sweepback angle = angle that trace of chord midpoints makes with vertical ≈ 0

mean section shape = waterplane at load waterline

4. BASIC WING THEORIES FOR ELLIPTICAL PLANFORMS

For infinite aspect ratio,

$$C_\ell = 2\pi\alpha \tag{8}$$

where C_ℓ = section lift coefficient.

The Lanchester-Prandtl wing theory [1] applies to wings having elliptical spanwise distributions of lift and aspect ratios larger that about 3. To relate finite and infinite aspect ratios at constant lift coefficient,

$$\alpha = \alpha_o + (C_L/\pi A) \tag{9}$$

where α = angle of attack for finite A

α_o = angle of attack on a section, infinite A

C_L = wing lift coefficient

$$\alpha = \alpha_o + (C_\ell/\pi A) = \alpha_o(1 + \frac{2}{A}) \tag{10}$$

In the linear range of lift coefficient versus angle of attack,

$$C_L = (\partial C_L/\partial\alpha)\alpha \ , \ (\partial C_L/\partial\alpha) = C_L/\alpha \tag{11}$$

$$C_\ell = (\partial C_\ell/\partial \alpha_o)\alpha_o \;, \; (\partial C_\ell/\partial \alpha_o) = C_\ell/\alpha_o \tag{12}$$

At $C_L = C_\ell$

$$(\partial C_L/\partial \alpha)\alpha = (\partial C_\ell/\partial \alpha_o)\alpha_o \tag{13}$$

$$(\partial C_L/\partial \alpha)\alpha_o(1 + \frac{2}{A}) = (\partial C_\ell/\partial \alpha_o)\alpha_o \tag{14}$$

$$(\partial C_L/\partial \alpha)(1 + \frac{2}{A}) = (\partial C_\ell/\partial \alpha_o) \qquad \text{(slopes)} \tag{15}$$

$$(C_L/\alpha)(1 + \frac{2}{A}) = (C_\ell/\alpha_o) \tag{16}$$

At $\alpha = \alpha_o$

$$C_L = C_\ell(\alpha/\alpha_o)(1/1 + \frac{2}{A}) = (C_\ell/1 + \frac{2}{A}) = \frac{2\pi\alpha}{1 + 2/A} \tag{17}$$

The Jones theory, for A less than .5, is

$$C_L = \frac{\pi}{2}\alpha A \tag{18}$$

Between $.5 < A < 3.$, tip vortices give a downward component to the inflow velocity, thereby decreasing the inflow angle α. The expressions for finite aspect ratio lift coefficient are applicable only to flat plates with ellipti-

cal or similarly shaped planforms.

5. EXAMINATION OF WING SECTION PROPERTIES

Although the wing-ship analogy treats the hull as a low-performance fin, it is possible that section properties have similar effects on hulls and on wings. To pursue this possibility, the effects of maximum section thickness ratio (y/c) and position of maximum section thickness (x/c) were examined. The results were compared to data for three series of ships, and a general agreement was found between the effects of y/c on wing sections and the effects of B/L on hulls.

From section characteristics [1,15] (Figure 4),

$$C_L'' = \partial C_L''/\partial\alpha = 2\pi[1.4 - \frac{x}{c}][.94 + .8\frac{y}{c}] \tag{19}$$

$(.03 < y/c < .11)$

$$x/c = \text{LCB from bow}/L \tag{20}$$

$$y/c = \frac{1}{2}B/L \tag{21}$$

Thus,

$$\partial C_L''/\partial\alpha = 2\pi[1.4 - \frac{LCB}{L}][.94 + .4\frac{B}{L}] \tag{22}$$

$(.06 < B/L < .22)$.

No ship data has been found to prove or disprove the validity of the factor for LCB location. Only the factor for section thickness can be examined in this report.

$$C_L' = L/\tfrac{1}{2}\rho V^2 L^2 \tag{23}$$

$$C_L'' = L/\tfrac{1}{2}\rho V^2 LT \tag{24}$$

$$C_L' = C_L'' \frac{T}{L} \tag{25}$$

A model series [12] specifically designed to yield data on variation of maneuvering characteristics with B/L had a slope of $\partial C_L''/\partial\alpha$ versus B/L of about $1/2\pi$, rather than 0.4 from the section data. Other model series were not consistent, but the general trend was to support a positive slope within each series, with roughly the same coefficient.

DATCOM

Designation NACA	Table 4.1.1-A C_{ℓ_α}(per °)	C_{ℓ_α}(per rad)	From Abbott & von Doenhoff C_{ℓ_α}(per rad)	y/c	x
0006	.108	6.188	6.215	3.001	30
0009	.109	6.245	6.011	4.501	30
63-006	.112	6.417	6.215	3.000	35
009	.111	6.360	6.071	4.500	35
012	.116	6.646	6.322	6.000	35
015	.117	6.704	6.322	7.500	35
018	.118	6.761	6.366	9.000	35
021	.118	6.761	6.548	10.500	35
64-006	.109	6.245	6.112	2.995	40
009	.110	6.303	6.388	4.490	40
012	.111	6.360	6.548	5.981	40
015	.112	6.417	6.388	7.482	35
018	.111	6.360	6.279	8.979	35
021	.110	6.303	6.433	10.481	35
65-006	.105	6.016	6.051	2.998	40
009	.107	6.131	6.031	4.496	40
012	.110	6.303	6.112	5.997	40
015	.110	6.303	6.279	7.498	40
018	.100	5.730	6.011	8.999	40
021	.112	6.417	6.548	10.499	40
66-006	.100	5.730	6.112	3.000	45
009	.103	5.901	6.112	4.499	45
012	.106	6.073	6.112	6.000	45
015	.105	6.016	5.821	7.495	45
63A010	.105	6.016	6.011	4.995	35
64A010	.110	6.303	6.011	4.995	40

Data for $\partial C_L/\partial\alpha$ Dependence on ($\frac{1}{2}$ thickness/chord) and location of Maximum Section Width

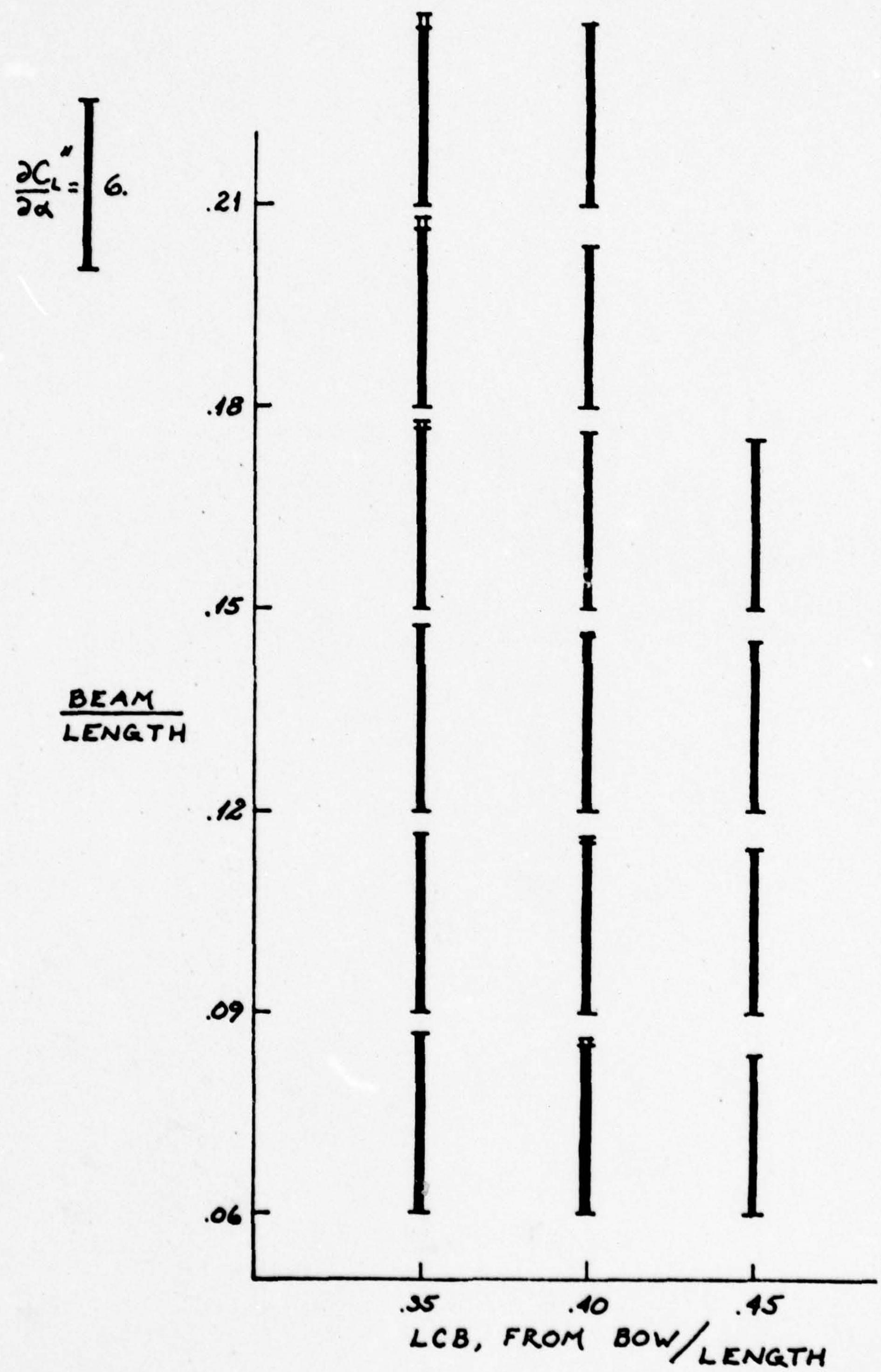

Figure 4: Lift-Slope $\partial C_L''/\partial\alpha$ versus B/L, LCB, for DATCOM Section

6. Y_v' versus B/L

Tests by Gerritsma, Beukelman, and Glansdorp [12] on a special set of Series 60 hulls showed a definite increase of Y_v' with increase of B/L beyond a value of about .05 (L/B = 20). Even after the effects of drag were subtracted, the tests still showed an increase of $\partial C_L'/\partial\alpha$ with increase of B/L. The slope for Y_v' versus B/L was about .018 - .014/.2 = .02 at Fn = .15. The slope for $\partial C_L'/\partial\alpha$ versus B/L was approximately .01.

The MARAD Series [13] showed little or no increase of Y_v' with increase of B/L. Examples were:
.00670 - .00645/.200 - .167 = .0075 and
.0126 - .0124/.200 - .181818 = .011.

The original Jacobs Series 60 [18] without propellers or rudders actually showed decrease of Y_v' with increase of B/L. The slope was -(.01387 - .01264)/.1666 - .125 = -.03. However, the Jacobs and Eda [11] Series 60 for the same hulls with propellers and rudders produced a slope of .01643 - .01509/.1666 - .125 = .032.

7. Y_v' versus C_B or C_P

Some small increase in Y_v' is to be expected for increase in C_B, just from the increase in drag on a fuller form hull. However, the drag contribution to Y_v' is small anyway, so a small addition may not be noticed. Another contribution to Y_v' arises from the change in hull shape.

The MARAD Series [13] best illustrates the effects of C_B variation within a consistent series of hull forms (Figure 6). When C_B increases, L_M/L (parallel midbody/total length) increases proportionally. This may cause an increase in Y_v' because it increases the length over which midship section bilge radius occurs and it increases the length of bottom having midship section bottom width. Fore and aft of the parallel midbody, the curvature from flat bottom to sides increases in radius, and the width of flat bottom tapers to zero at the ends. Two effects then augment each other. The greater extent of minimum bilge radius makes the hull more like a thick foil with small radius edges. The greater extent of full width bottom creates more skin friction resistance to cross-flow, since such flow will have greater distances to traverse fore and aft of the former ends of parallel midbody.

The series of elongated bodies of revolution [20] also

have increasing lift with increasing C_B, probably because the fuller shape has more skin friction resistance to transverse flow, and presents more lateral area within the confines of $d \times \ell$.

The results of several series, when compared series against series, show that gross increases in C_B with accompanying changes in other characteristics, generally lead to decreases in Y_v'. The full form tanker hulls, such as the MARAD Series, the HyA tankers [5,8], and the Glansdorp and Pijfers tankers [14], lie well below the Eda destroyers, and below the Series 60 hulls on the Y_v' versus A plots. Furthermore, the finer-formed series are less consistent in their dependence of Y_v' on C_B. This may occur because the increases in C_B decrease the slenderness of the ends, cut down on deadwood area, and decrease lift generation at the ends, especially the sterns.

8. PROPELLER EFFECTS

Propellers are known to contribute to directional stability. Their effect on Y_v' is measurable, as can be seen from comparison of powered and non-powered model test results. One form has been suggested from submarine analysis by Abkowitz (under the assumption that the propeller is operating near the point of maximum efficiency, $\partial\eta/\partial J = 0$, behind a streamlined body):

$$\Delta Y_v' = -\frac{1.8d^2}{L^2}(1 - w_f)\left(\frac{1}{2\pi\eta}\right)\left(K_T - J\frac{\partial K_T}{\partial J}\right) \qquad (26)$$

d = propeller diameter

J = advance coefficient V_A/nd

K_T = thrust coefficient = $T/\rho n^2 d^4$

L = ship length (Lbp)

η = propeller efficiency

n = RPM

ρ = density of seawater

T = thrust of propeller

V = speed of ship

V_A = speed of advance of propeller

w_f = wake fraction = $(V - V_A)/V$

Unfortunately for this study, the data necessary to calculate $\Delta Y_v'$ are not available in the data sets used.

Thus the formula is useful only as a suggested form without experimental verification for ship hulls.

A formula of this type would be desirable for evaluating the differences in Y_v' attributable to various propeller parameters, such as power per propeller and number of propellers. It is desirable to have a breakdown of contributions to Y_v' rather than to have some simple formula for overall Y_v' which is invariant with changes in basic parameters other than aspect ratio.

Sample Calculation for Propeller in Free Stream

$$\Delta Y_v' = -\frac{1.8d^2}{L^2}(1 - w_f)\left(\frac{1}{2\pi\eta}\right)\left(K_T - J\frac{\partial K_T}{\partial J}\right)$$

$L = 450$ ft.

$T = 27$ ft.

$d = .7\ T$

$Fn = .20$

$V = .20 \times \sqrt{32.2 \times 450} = 24$ ft/sec.

$= 14.2$ knots

$EHP = 2800\ hp = R_T V/550 = (1 - t)TV/550$

$w_f = .3$

$J = V_A/nd = 24 \times .7/1 \times 27 \times .7 = .9$

$K_T = T/\rho n^2 d^4 = EHP \times 550/(1 - t)V\rho n^2 d^4$

$= 2800 \times 550/(1 - .2) \times 24 \times 2 \times 1^2 \times (27 \times .7)^4$

$= .3$

$\frac{\partial K_T}{\partial J}$ assume $-.3$

$$\Delta Y_v' = -1.8\,\frac{(27 \times .7)^2}{450^2}\,(1 - .3)\left(\frac{1}{2\pi \times .6}\right)[.3 - .9 \times (-.3)]$$

$= .00034$

The propeller operates in water which has been disturbed by the passage of the hull, and in general the water around the stern has a forward motion acquired by its interaction with the movement of the ship. The forward-moving water is called the wake, and it results in the propeller advancing relative to the water at some speed V_A (speed of advance) which is a lower speed than the ship speed V.

The difference between ship speed V and speed of advance V_A is called the wake speed. Taylor introduced "wake fraction" = w_f:

$$w_f = (V - V_A)/V \tag{27}$$

$$V_A = V(1 - w_f) \tag{28}$$

The propeller, when developing thrust, accelerates the water ahead of it, thereby lowering the pressure around the stern and increasing the velocity of the flow around the stern. The effect of the propeller in inducing an inflow velocity reduces the forward wake somewhat below the nominal wake for bare hull.

When a hull is towed, there is an area of high pressure over the stern which has a resultant forward component

reducing the total resistance. With a self-propelled hull, the pressure is reduced over some of the stern area by the action of the propeller in accelerating the water flowing to it. The result is that the forward component of the pressure is reduced, the resistance is increased, and the thrust necessary to propel the ship at a given speed is increased. The common practice is to view this increase in resistance as a decrease in the thrust available at the propeller, so that although the screw provides thrust T, only thrust R_T is available to overcome resistance. The "thrust deduction fraction" = t:

$$t = (T - R_T)/T \tag{29}$$

$$R_T = (1 - t)T \tag{30}$$

$(1 - t) \equiv$ thrust deduction factor

The net result, the ratio of work done on the ship to that done by the screw, is hull efficiency η_H:

$$\eta_H = P_E/P_T = R_T V/TV_A = (1 - t)/(1 - w) \tag{31}$$

EFFECT OF BLOCK COEFFICIENT ON WAKE FRACTION (w) AND THRUST DEDUCTION FRACTION (t)

Series 60 (from [9,25])

LCB	2.5A	2.5A	1.5A	1.5A	2.0A	.5A	.5A	.5A
C_B	.60	.65	.60	.65	.70	.60	.65	.70
w	.285	.310	.246	.263	.316	.230	.252	.274
t	.179	.206	.177	.167	.204	.154	.155	.161
η_H	1.148	1.151	1.093	1.130	1.164	1.098	1.129	1.156

LCB	.5F	.4F	.5F	.5F	.8F	1.4F	1.5F	1.5F	1.5F
C_B	.60	.65	.70	.75	.80	.65	.70	.75	.80
w	.218	.247	.271	.367	.363	.229	.255	.311	.362
t	.140	.160	.180	.227	.330	.136	.156	.171	.238
η_H	1.10	1.116	1.125	1.221	1.053	1.121	1.133	1.203	1.195

LCB	2.5F	2.6F	2.5F	3.5F	3.5F
C_B	.70	.75	.80	.75	.80
w	.259	.297	.355	.288	.355
t	.164	.170	.200	.176	.170
η_H	1.128	1.181	1.240	1.157	1.287

Wake fraction and thrust deduction fraction generally increase with C_B. The hull efficiency generally increases with C_B since w is more affected than t. Hence, the anticipated increase in resistance for higher C_B is somewhat offset by increased hull efficiency. But since t increases with C_B, the effect of the propeller in reducing pressure over the stern and pulling the streamlines more toward the propeller, increases with C_B. The effect of the streamline modification may be to increase the lateral area over which the transverse velocity components due to sideslip can generate lift, thereby increasing transverse lift and the coefficient Y_v'.

This may help to account for the large augmentation to Y_v' by propeller action, as found by Glansdorp and Pijfers for full tanker models. The $\Delta Y_v'$ that they found was much larger than the $\Delta Y_v'$ predicted from analysis of propellers in a free stream. The effect of the thrust deduction phenomenon may be an explanation for the discrepancy.

9. RUDDER EFFECTS

Jacobs Series 60, Model 2,1,1

$L = 5.0$ ft.	$L/B = 7.0$
$B = .714$ ft.	$B/T = 2.68$
$T = .267$ ft.	$L/T = 18.75$
Rudder span = .200 ft.	Area = .021 ft.^{2}
Rudder chord = .105 ft.	Aspect ratio = 2span/chord = 3.81

$$.2 \times .105/5.0 \times .267 = .0157$$

For this value of A, $\partial C_L/\partial\alpha \simeq 2\pi/(1 + 2/A) = 4.12$ or 4.

$$\text{Lift} = C_L \times \frac{1}{2}\rho A U^2$$

$$C_L = (\partial C_L/\partial\alpha)\alpha = (\partial C_L/\partial\alpha)(V/u_s)$$

$\Delta Y_v{}' = (\partial C_L{}'/\partial\alpha) + D_o{}'$ but $D_o{}'$ is negligible.

Therefore, using $\Delta Y' \simeq C_L{}'$

$$\Delta Y_v{}' = C_L{}'/V$$

$$\Delta Y_v{}' = \left(\frac{\partial C_L}{\partial\alpha}\right)\left(\frac{V}{u_s}\right)\left(\frac{1}{V}\right)\frac{\frac{1}{2}\rho\frac{S \times C}{T \times L} \times T \times L\,[U \times (1 - w)]^2}{\frac{1}{2}\rho L^2 U}$$

$$= 4 \times \frac{1}{U \times (1 - w)}\,\frac{\frac{1}{2}\rho\, .2 \times .105\,[U \times (1 - w)]^2}{\frac{1}{2}\rho L^2 U}$$

$$= \frac{4 \times 1 \times .2 \times .105 \times .7}{5^2} = .00235$$

Model	1,1,1	2.1,1	2,1,2	2,1,3	3,1,4
Span	.2	.2	.2	.2	.2
Chord	.105	.105	.167	.080	.105
L	←		5 feet		→
T	.267	.267	.267	.267	.267
A	3.81	3.81	2.4	5.	3.81
$\partial C_L/\partial \alpha$	4.1	4.1	3.4	4.5	4.1
$\Delta Y_v'$	.0024	.0024	.0032	.0020	.0024

Model	4,1,1	5,1,1	6,1,1	7,1,1	8,1,1
Span	.2	.164	.258	.2	.2
Chord	.105	.105	.105	.105	.105
L	←		5 feet		→
T	.267	.2175	.345	.267	.267
A	3.81	3.12	4.91	3.81	3.81
$\partial C_L/\partial \alpha$	4.1	3.8	4.5	4.1	4.1
$\Delta Y_v'$	.0024	.0018	.0034	.0024	.0024

Jacobs' Models, Simplified Calculation for Rudder Effect on Y_v

EFFECTS OF RUDDERS AND PROPELLERS

Comparing a series of bare hulls versus a series of hulls with propellers and rudders, all running at Fn = .20,

Jacobs Models	2,1,1	2,1,2	2,1,3	3,1,1	4,1,1
Y_v'	.01627	.01659	.01563	.01643	.01509
	2	2	2	3	4
Y_v'	.01307	.01307	.01307	.01264	.01387
$\Delta Y_v'$	.00320	.00352	.00256	.00379	.00122
Calculated Rudder $\Delta Y_v'$	.0024	.0032	.0020	.0024	.0024
Calculated Propeller $\Delta Y_v'$	.00034	.00034	.00034	.00034	.00034
Total	.0027	.0035	.0023	.0027	.0027

Jacobs Models	5,1,1	6,1,1	7,1,1	8,1,1
Y_v'	.01130	.02669	.01787	.01723
	5	6	7	8
Y_v'	.00943	.02172	.01531	.01365
$\Delta Y_v'$	.00187	.00497	.00256	.00358
Calculated Rudder $\Delta Y_v'$	.0018	.0034	.0024	.0024
Calculated Propeller $\Delta Y_v'$	.00034	.00034	.00034	.00034
Total	.0021	.0037	.0027	.0027

With one exception, the simple rudder calculation accounts for 70% or more of the total $\Delta Y_v'$ measured. In one case, it overpredicts. The free stream propeller calculation is inadequate to make up for the difference in most cases. It is reasonable to state that the formula is not applicable to cases where propellers operate aft of blunt sterns. However, there is not data available to examine the applicability of the formula to transom sterns, where the propellers have nearly free stream operation.

10. INTERACTION OF PROPELLERS WITH RUDDERS

Mandel [9] and others have shown that the propeller race makes rudders more effective as ship-turning devices. The same wake-straightening effect that causes propellers to develop transverse lift also increases the angle of attack on a deflected rudder mounted aft of the propeller. Additionally, the increased flow velocity within the race helps a rudder to develop more lift. Proof of the effect on the rudder's ship-turning ability can be seen in Figure 10, where increased propeller RPM increases Y_δ.

The wake-straightening effect of the propeller works to reduce the rudder's dynamic stability effectiveness. With the rudder fixed at zero deflection, any straightening effect on the inflow due to the propeller race reduces the angle of attack on the rudder. The situation becomes complicated by the nature of the wake straightening. Because the fluid flow is a continuous phenomenon, the wake does not straighten immediately aft of the propeller. The effect is gradual, increasing with distance aft of the propeller. Evidence of the confounding nature of the phenomenon comes from four sources.

Jacobs found on Series 60 model 2 that $\Delta Y_v'$ varied consistently with rudder chord variation. The variation was non-linear; the slope of $\Delta Y_v'$ versus chord length

decreased with increasing chord length. Presumably, the chord length additions were made to the trailing edge, where the wake was more straightened, hence the additions became less useful.

Eda found on destroyer models that Y_v' decreased with increasing Froude number, hence speed. Destroyers have nearly free stream flow to the propellers, so the increase in Y_v' due to propellers that occurs for full form ships will not be as large for destroyers. The high power destroyers have considerable wake straightening due to propellers, so the effectiveness of rudders naturally decreases with increasing Fn, as the wake is further straightened.

Glansdorp and Pijfers used two hulls and two sets of rudders, and found that increasing rudder chord decreased Y_v' at corresponding RPM. "...increasing the rudder area not necessarily gives a better course stability," because other things remaining fixed, a decrease in Y_v' decreases course stability. Since the propeller RPM did not vary, the contribution to Y_v' due to a propeller operating behind a full stern also did not vary. The decrease in Y_v' then can be attributed to the shift of rudder area aft when the chord was increased, which shift put the rudder in more straightened wake and decreased its utility as a course

stabilizing device. Since increased chord length reduced the aspect ratio of the rudders, a reduction of rudder effectiveness could have occurred regardless of the flow straightening effect of the wake.

Surber [24] tested a transom stern patrol craft with various spade rudders, and found that the tactical diameter of scheme 3 (rudder area = 93 ft.^{2}, A = 1.80) was less than that of scheme 2 (rudder area = 101 ft.^{2}, A = 1.46). The improved Y_δ for the smaller rudder apparently was due to its higher aspect ratio and its higher percentage of area in the propeller slipstream. The scheme 2 rudder had a long chord and short span, reaching just below the propeller shaft. The scheme 3 rudder had a shorter chord and longer span, reaching well below the propeller shaft. The improvement in Y_δ occurred despite the fact that the scheme 2 rudder area was slightly aft of the scheme 3 rudder area, which should have placed the scheme 2 rudder in more straightened flow and should have improved its Y_δ.

It is evident that a trade-off arises between Y_δ and Y_v. If a designer wants a ship with small tactical diameter, he should place the rudder at a point well aft of the propeller to take advantage of the flow-straightening. If instead he wants a dynamically stable ship, he needs as little flow-straightening as possible affecting the rudder,

so he should place the rudder as close as possible to the propeller, or he should try another approach by using twin rudders placed well to the side of the propeller slipstream.

It is not sufficient to depend on variations of rudder area alone to properly effect changes in Y_δ or Y_v. The designer will need to evaluate the flow conditions to the rudder and propeller as well as the characteristics of such devices.

[Note: In the previous discussions of rudders and their interaction with the hull and with propellers, the linearized equations of motion from Strom-Tejsen [23] have been the source for the coefficients Y_v and Y_δ. In the non-linear equations, the Taylor expansion would lead to use of cross-coupled coefficients such as $Y_{v\delta\delta}$ and $Y_{\delta vv}$ since both δ (rudder) and v (ship) are involved simultaneously in a non-linear treatment of maneuvering.]

11. SKEGS

Several authors treat skegs as isolated lifting surfaces, using skeg effects as linear additions to the basic hull stability derivatives. It is to be expected that rudders and short skegs may act as such lifting devices. They stick abruptly into the flow, through or beyond the boundary layer. Because of their small size, they do not have a profound effect on the boundary layer nor on the vortices being developed by the hull. However, large, faired-in skegs or deadwood do have a profound effect on the basic flow conditions. Saunders' photographs show this well. Jacobs found that large areas of deadwood and fairing could augment the basic hull lift coefficient on Taylor Series 840 hulls by a factor of 2. However, it is not likely that such a convenient factor would apply to skegs on other hulls. Glansdorp and Pijfers found a much smaller effect on full tanker models. Destroyer hulls might have even a larger figure because their basic sterns are so smoothly cut away from somewhere aft of midship to the transom stern. Unfortunately, no data has been found to support this statement. Furthermore, no data has been found to examine the effects of small changes in existing skegs on Y_v. It is likely that the skeg effect on Y_v is linear with

skeg changes over a small range, but no proof has been found.

12. DATA SETS

Elongated Body of Revolution [20]

The results of experiments on elongated bodies of revolution show how important bow, stern, and bottom shape can be for generation of lift. The hulls had circular sections, no deadwood, blunt bows, and tapered sterns.

$C_P = \nabla/(\pi d^2/4)\ell$

d = diameter

ℓ = length

$L' = \partial C_L'/\partial\alpha = L/\frac{1}{2}\rho U^2 \ell^2$

$Y_v' = L' + D_o'$

D_o' = unknown, assumed small

d/ℓ (taken as aspect ratio)	L' (C_P = .55)	L' (C_P = .65)
.1	.0054	.0063
.125	.0076	.0091
.143	.0096	.0111
.167	.0124	.0141
.2	.0166	.0189
.25	.0233	.0267

The plots of L' versus A fall well below the plots for

ships and flat plates, Figure 11. This is to be expected because there are no lift generation devices at the stern or the bow and the middlebody presents a shape that the fluid flows under very easily. With regard to bow and stern lift generation, Landweber and Johnson pointed out that such effects cannot be treated as independent from the effects of the bare hull. There is too much interaction effect with the boundary layer to treat skegs and deadwood as isolated lifting surfaces.

Landweber and Johnson found that bodies of revolution have a relation between lift and angle of attack similar to that found by Bollay for flat rectangular plates: "At small angles of attack α, the lift of a body of revolution is expressible in the form $L = C_1\alpha \dot{+} C_2\alpha^2$. It is well known that a very long cylinder at an angle of attack is subject to a normal force proportional to $\sin^2\alpha$, an effect which may be explained by assuming that the longitudinal and transverse components of the incident flow act independently. [Bollay's two-dimensional flow across the span] It appears reasonable to suppose that this effect accounts for the quadratic term at small angles of attack."

Special Series 60

Gerritsma, Beukelman, and Glansdorp tests on Series 60 [12].

(For original Series 60 [25], $6.5 < L/B < 8.5$).

B/L	.25	.181818	.14286	.1	.05	0
L/B	4	5.5	7	10	20	∞
L(m)	3.048	3.048	3.048	3.048	3.048	3.048
B(m)	.762	.5542	.4354	.3048	.1524	.006
T(m)	.1742	.1742	.1742	.1742	.1742	.1742
C_B	.70	.70	.70	.70	.70	1.0
A = 2T/L	.114	.114	.114	.114	.114	.114
$-Y_v'$(Fn = .15)	.018	.017	.016	.0145	.014	.015
$-Y_v'$(Fn = .2)	.0185	.0176	.0175	.015	.014	.016
$-Y_v'$(Fn = .3)	.0245	.023	.0207	.0176	.0145	.016

Norrbin formula: $Y_v' = -1.69\pi\ (T^2/L^2) - .08\ (BT/L^2)C_B$

	.01734	.01734	.01734	.01734	.01734	.01734
	.00080	.00058	.00046	.00032	.00016	.00001
Y_v'	.01814	.01792	.01780	.01766	.01750	.01735

Slope of Y_v'(Fn = .15) is about (.018 - .014)/(.25 - .05) = .02

Slope of $\partial C_L'/\partial\alpha$ is assumed to be about .01

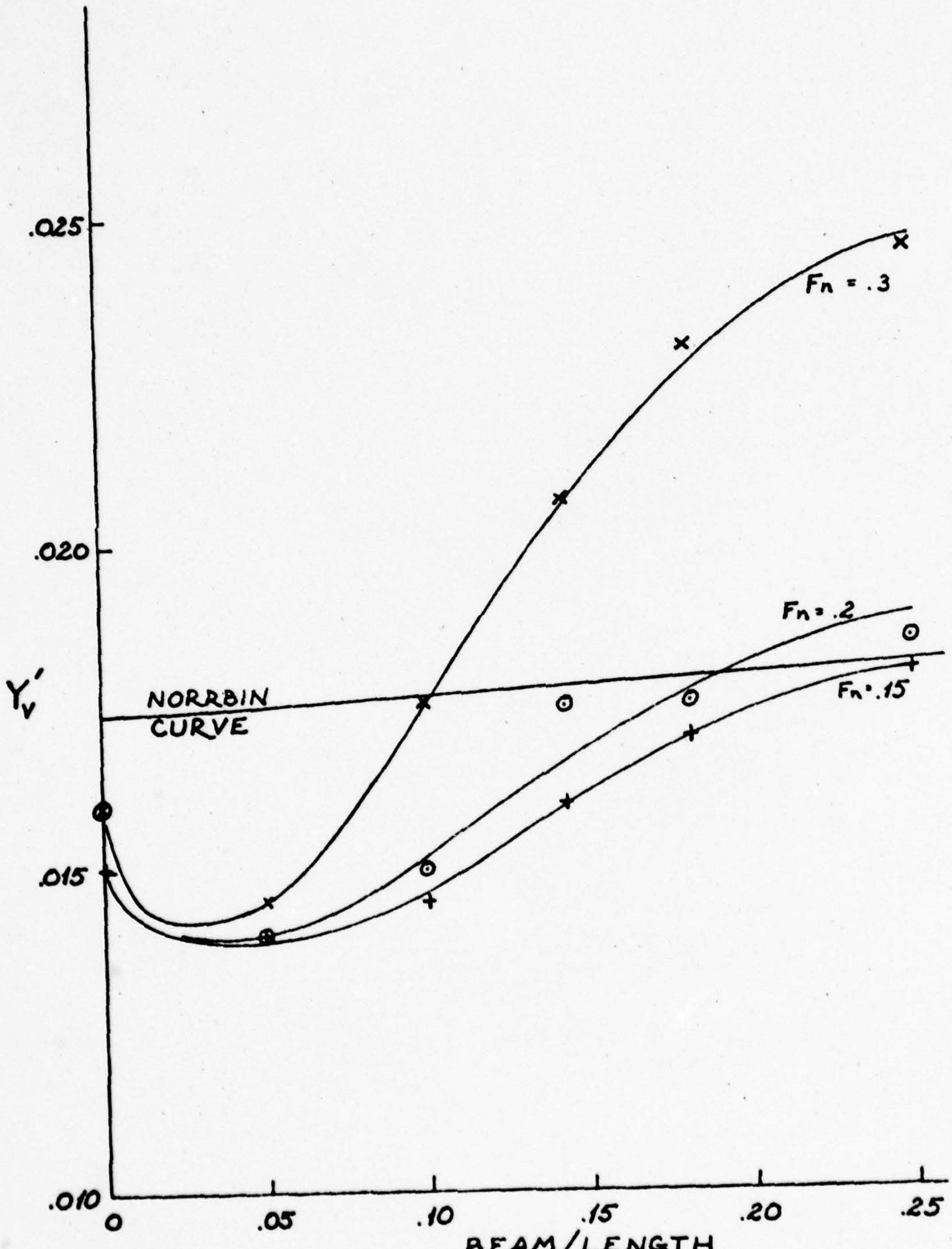

Figure 5: Y_v' versus B/L for Special Series 60

Effect of Drag, D

$D = \frac{1}{2}\rho V^2 S\, C_D(R,\ B/L)$

$C_D = C_F + C_R$

$C_F = C_F(R)$

For Special Series 60,

Fn	.15	.2	.3
$V = Fn\sqrt{gL}$	2.69	3.59	5.38 ft/sec
$Re = VL/\nu$	2.69×10^6	3.59×10^6	5.38×10^6
C_F	.0040	.0038	.0036

where C_F is non-dimensionalized on surface area.

Roughly, surface area = $LT\pi$.

To non-dimensionalize on projected area, LT, C_F must be multiplied by π. Further, to non-dimensionalize on L^2, C_F must be multiplied by T/L.

$C_F' = C_F\pi(T/L)$

C_F'	.00072	.00068	.00065
Approximate C_R'	.0001	.0003	.0009
C_D'	.0008	.001	.0016

Both C_R' and surface area are increasing functions of B/L. Thus, C_D is a function of speed and B/L ($C_D(R,B/L)$ as above). The slope of C_D' versus B/L is positive, and $\partial C_L'/\partial\alpha = Y_v' - C_D'$ should have lesser slope than Y_v'.

MODEL	A	B	C	D	E	F	H	K	I	O	M	L	J	G	N	P
A = 2T/L	0.121	0.111	0.103	0.148	0.133	0.121	0.103	0.107	0.089	0.097	0.082	0.089	0.074	0.133	0.107	0.089
B/L	0.182	0.167	0.154	0.222	0.200	0.182	0.154	0.200	0.167	0.182	0.154	0.200	0.167	0.200	0.200	0.200
B/T	3.000	3.000	3.000	3.000	3.000	3.000	3.000	3.750	3.750	3.750	3.750	4.500	4.500	3.000	3.750	4.500
C_B	0.875	0.875	0.875	0.850	0.850	0.850	0.850	0.850	0.850	0.875	0.875	0.850	0.850	0.800	0.800	0.800
L_M/L	0.537	0.537	0.537	0.443	0.443	0.443	0.443	0.443	0.443	0.537	0.537	0.443	0.443	0.251	0.251	0.251
$-Y_v' \times 10$ Bare Hull	.1285	.105	.0875	.202	.1575	.124	.0850	.0955	.0645	.0810	.0570	.0670	.0470	.145	.0895	.0630
$-Y_v' \times 10$ Standard Rudder-Propeller Comb.	.1513	.1268	.1141	.235	.192	.1553	.1165	.1294	.0895	.1022	.0795	.0935	.0666	.1852	.12	.0874

MARAD SERIES [13]

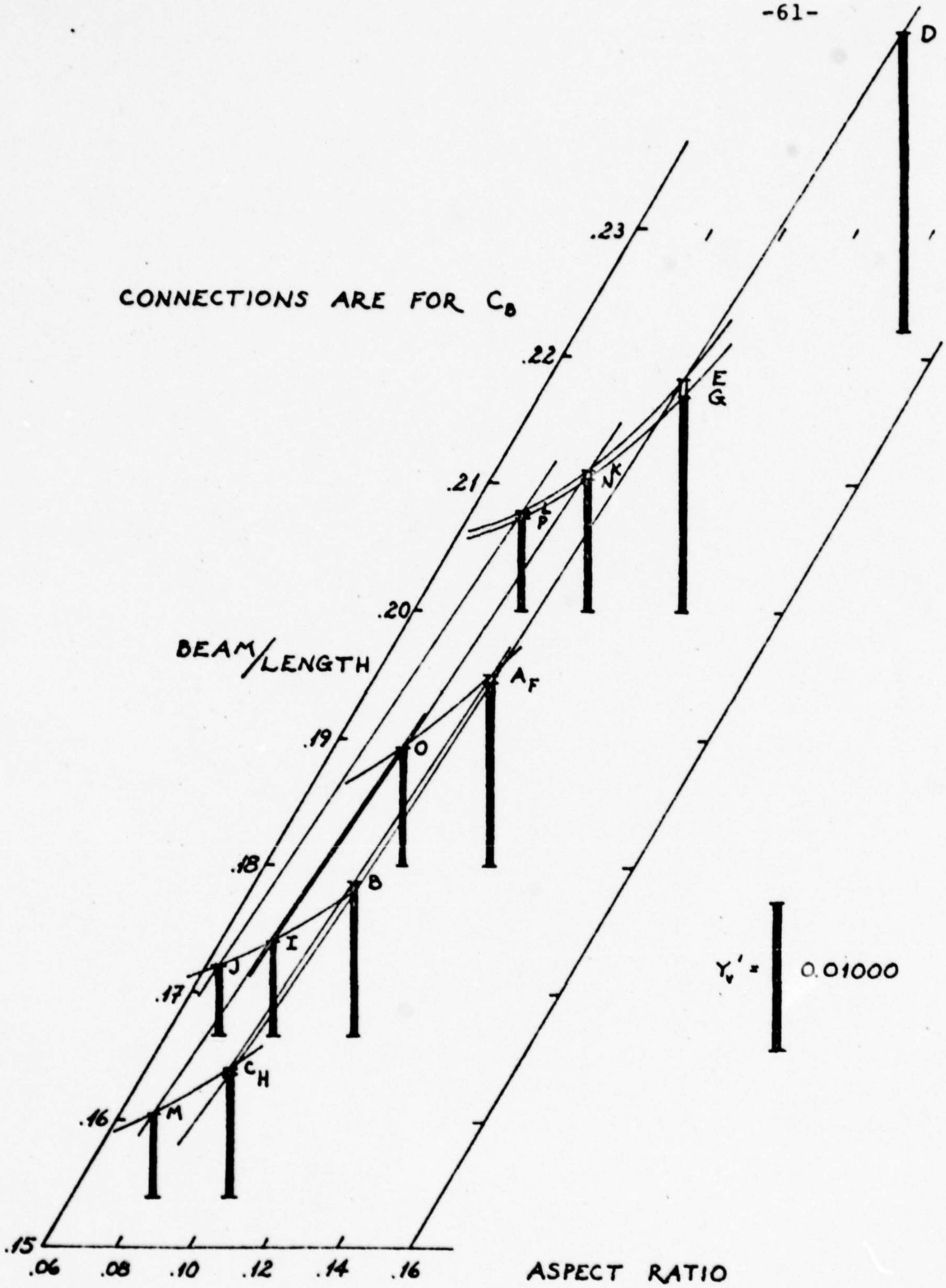

Figure 6: Y_v' versus B/L, A, and C_B for MARAD Series

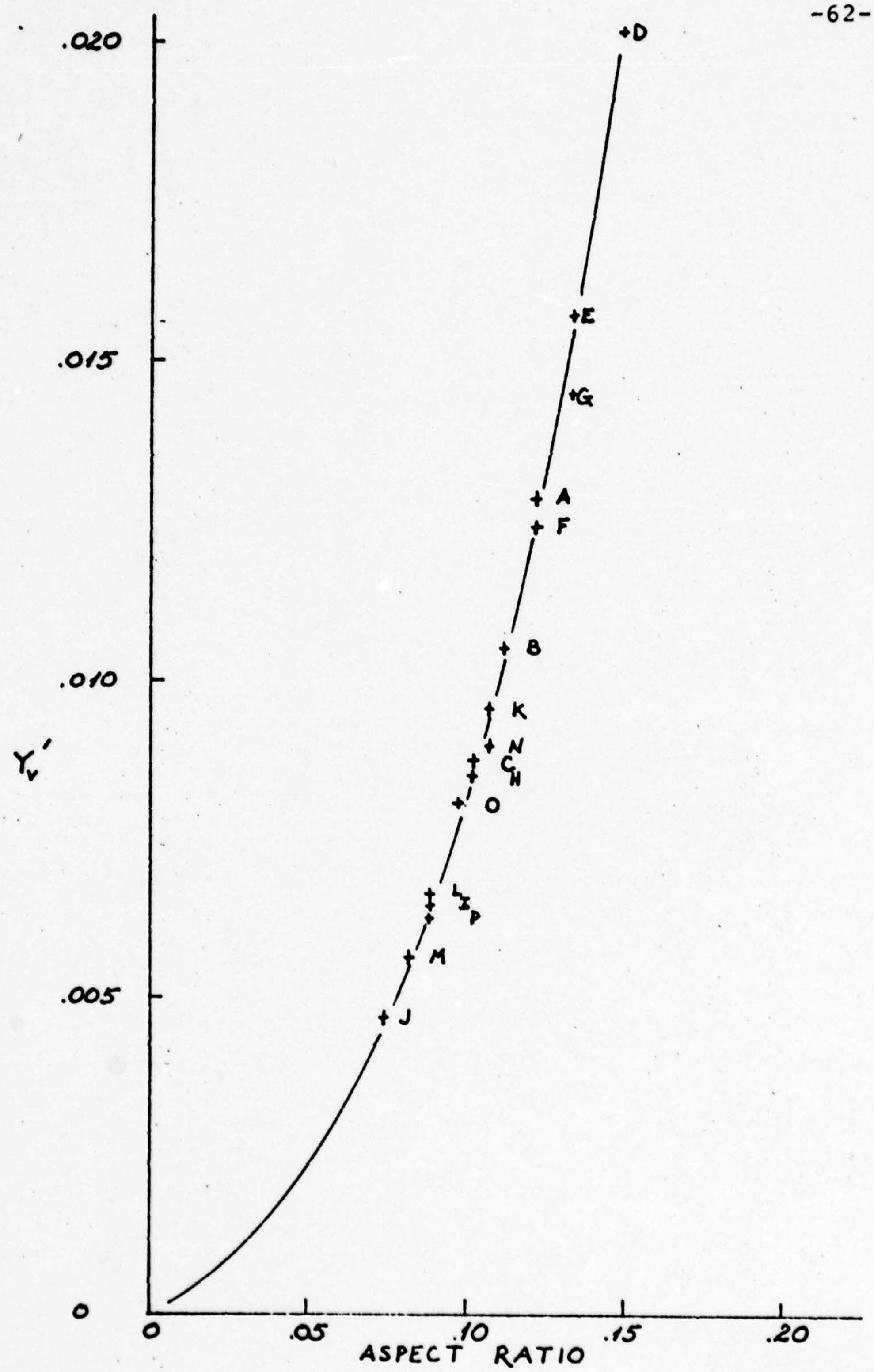

Figure 7: Y_v' versus A for MARAD Series

Bare Hull from Jacobs Series 60 [18]

$Y_\beta" = L_\beta" + D_o"$

MODEL	2	3	4	5	6	7	8
$D_o"$	0.015	0.017	0.014	0.017	0.015	0.019	0.021
$Y_\beta"$	0.245	0.237	0.260	0.217	0.315	0.287	0.256
$L_\beta"$	0.230	0.220	0.246	0.200	0.300	0.268	0.235
B/T	2.68	3.12	2.34	3.28	2.07	2.68	2.68
B/L	0.1428	0.1667	0.125	0.1428	0.1428	0.1428	0.1428
L/B	7.0	6.0	8.0	7.0	7.0	7.0	7.0
L/T	18.75	18.75	18.75	23.0	14.5	18.75	18.75
LCG/L	0.515	0.515	0.515	0.515	0.515	0.505	0.475
C_B	0.6	0.6	0.6	0.6	0.6	0.7	0.8
C_P	0.614	0.614	0.614	0.616	0.614	0.713	0.807
C_A	0.9772	0.9772	0.9772	0.9740	0.9772	0.9818	0.9913
A	0.1067	0.1067	0.1067	0.0870	0.1379	0.1067	0.1067

Y_v'	.01307	.01264	.01387	.00943	.02172	.01531	.01365
$-D_o'$	.00080	.000910	.00075	.00074	.00103	.00101	.00112
$=L_v'$	0.01227	0.01173	0.01312	0.00870	0.02069	0.01429	0.01253
	2	3	4	5	6	7	8
A = 2T/L	0.1067	0.1067	0.1067	0.0870	0.1379	0.1067	0.1067

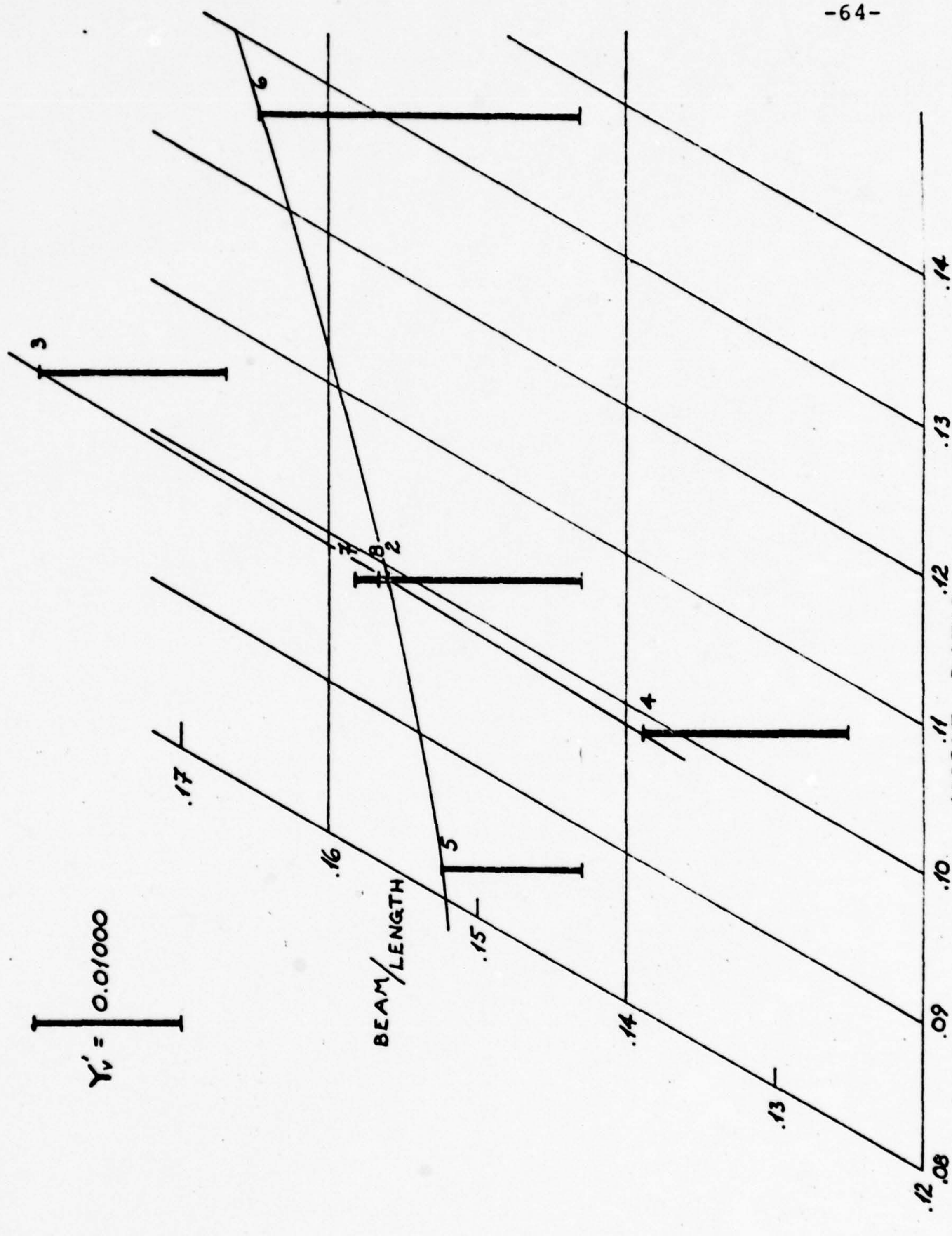

Figure 8: Y_v' versus B/L, A, and C_B for Jacobs' Series 60, Bare Hulls

Hull with Propellers and Rudders from Jacobs Series 60 [18]

MODEL	1,1,1	2,1,1	2,1,2	2,1,3	3,1,1	4,1,1	5,1,1	6,1,1	7,1,1	8,1,1
C_B	.6	.6	.6	.6	.6	.6	.6	.6	.7	.8
B/L	.1333	.1428	.1428	.1428	.1667	.125	.1428	.1428	.1428	.1428
A = 2T/L	.1067	.1067	.1067	.1067	.1067	.1067	.0870	.1379	.1067	.1067
L/T	18.75	18.75	18.75	18.75	18.75	18.75	23.00	14.50	18.75	18.75
$-D_o''$	.015	.015	.015	.015	.017	.014	.017	.015	.019	.021
$-D_o'$	.00080	.00080	.00080	.00080	.00091	.00075	.00074	.00103	.00101	.00112
$-Y_\beta''$	.255	.305	.311	.293	.308	.283	.260	.387	.335	.323
$-Y_v'$	.0136	.01627	.01659	.01563	.01643	.01509	.01130	.02669	.01787	.01723
Rudder Area	.021	.021	.0334	.016	.021	.021	.01722	.02709	.021	.021

Eda Series 60 Controllability Models [11]

MODEL	60B2	60	60R1	60R2	60B1	60B3	60H1	60H2	70	80
Rudder Area	.021	.021	.033	.016	.021	.021	.017	.027	.021	.021
$-Y_\beta''$	.270	.305	.311	.293	.308	.283	.260	.349	.324	.354
$-Y_v'$	.01440	.01627	.01659	.01563	.01643	.01509	.01130	.02407	.01728	.01888

C_B Series	60	70	80	L/T Series	60H2	60	60H1
L/B Series	60B3	60	60B1	Rudder Series	60R2	60	60R1

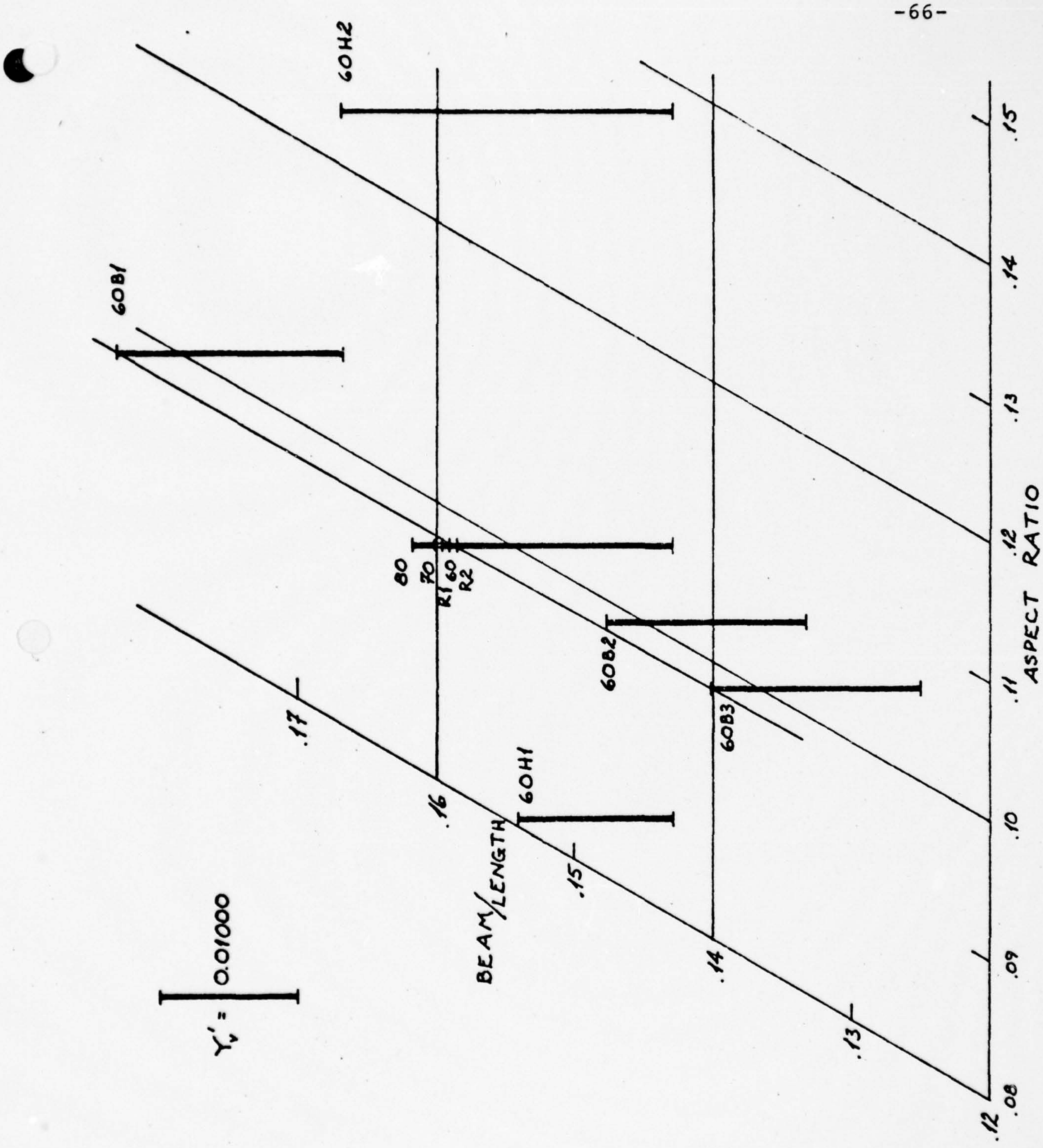

Figure 9: Y_v' versus B/L, A, and C_B for Eda's Series 60, with Propellers and Rudders

HyA Large Tanker Models, with Propellers and Rudders

MODEL	81000 m^3 [5]	190000 m^3 [8]
B	33.82 m	47.5 m
T	12.92 m	18.5 m
L	232.86 m	305 m
C_B	.80	.84
B/T	2.62	2.57
B/L	.145	.156
A	.111	.121
Y_v'	.01360	.01530

Simulated Self-Propelled Destroyer [7]

$B = 46$ ft.

$T \simeq 14$ ft.

$L = 440$ ft.

$C_B = .494$

$\Delta = 4000$ tons

$A = .0636$

$B/L = .1045$

$B/T = 3.3$

$Y_v' = .10149$

DD

This is data for a fictitious destroyer escort "study ship", synthesized from realistic data.

Navy AO177 Fleet Oiler [10]

(fully appended and propelled)

$L = 550$

$B = 88$

$T = 32.2$

$B/L = .16$

$B/T = 2.733$

$C_B = 27400 \times 35/550 \times 88 \times 32.2 = .615$

$2T/L = .1171$

$Y_v' = -.016046$

Mariner [9,23]

$L = 528$

$B = 76$

$T = 27$

$\Lambda = 19000$

$C_B = .61$

$B/L = .144$

$B/T = 2.8$

$2T/L = A = .1023$

$Y_v' = .011604$

<u>Eda Destroyers, Self-Propelled [11]</u>

Ship	DL-2					DD-692	
	S31	O31	S41	S51	O51	Fn = .15	Fn = .38
L/T	34					27.4	
A	.059					.073	
B/T	3.41					2.89	
B/L	.1004					.1055	
C_B	.51					.53	
Rudder Area	102.5 x 2					not listed	
Y_v'	.01049	.009205	.00866	.00819	.007424	.008591	.009389

S31	sonar dome, Fn = .20
O31	no dome, Fn = .20
S41	sonar dome, Fn = .34
S51	sonar dome, Fn = .40
O51	no dome, Fn = .40

Glansdorp and Pijfers - Full Tanker Models [14]

L = 310 m	B/L = .152
B = 47.16 m	B/T = 2.5
T = 18.90 m	A = 2T/L = .122
∇ = 235000 m^3	∇ = 232690 m^3

Rudders	Balanced I	Balanced II	Mariner-type III	Fixed Portion IV	Twin V
A_R	2.87	2.3	3.36	2.3	3.37
$Area_R$	75.4	115	78.8	115	38x2
$\frac{Area_R}{L \times T}$	.013	.02	.013	.02	.0065x2

\- - - - - -

SHIP	PROP & RPM	RUDDER	SKEG	$-Y_v'$
01				.01562
02	Y85	I		.01938
03		II		.01733
04	Y67	II		.01836
05	Y85	II		.01821
06	Y102	II		.01878
M1				.01438
M2			Yes	.01510
M3	Y85			.01600
M4	Y85		Yes	.01717

SHIP	PROP & RPM	RUDDER	SKEG	$-Y_v'$
M5		III		.01559
M6		III	Yes	.01619
M7	Y85	III		.01716
M8	Y85	III	Yes	.01825
M9		IV	Yes	.01663
M10	Y85	IV		.01762
M11	Y67	IV	Yes	.01768
M12	Y85	IV	Yes	.01813
M13	Y102	IV	Yes	.01829
M14		V	Yes	.01722
M15	Y85	V	Yes	.01832

	Bare Hull		Fully appended hull, average		
	01	M1	0	M	with skeg
$-Y_v'$	.01562	.01438	.01900	.01750	.01820

		Y_δ'			
Rudder		Propeller RPM			
	No Prop	67	85	102	
I	.00072	.00163	.00275	.00372	+
II	.00124	.00250	.00305	.00377	×
III	.00094	.00217	.00277	.00330	⊙
IV	.00127	.00275	.00344	.00411	△
V	.00057	.00169	.00208	.00237	⊡

Contribution $\Delta Y_v'$ due to propellers is .00162 which is about 10 times the number expected from Abkowitz's formula for propeller in a free stream. Apparently there is much more effect of a propeller on flow ahead of and behind the propeller plane on a full form ship than there is in a free stream.

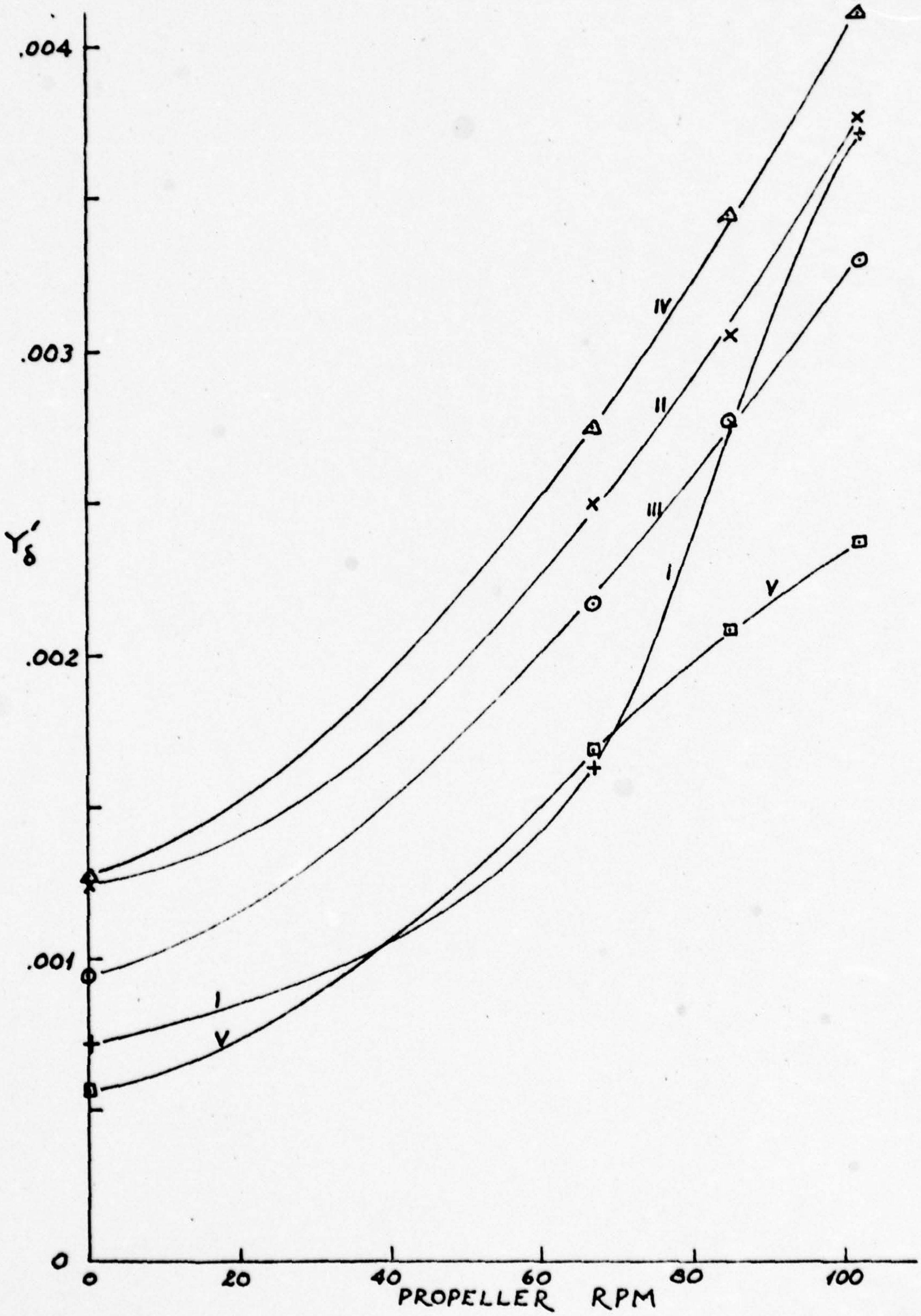

Figure 10: Y_δ' (for rudders) versus Propeller RPM for Full Tanker Models

13. CONCLUSION

A disappointingly small amount of data was available for analysis of transom stern vessels. Many more data were available for full form tankers, so most of the results are more applicable to that class of ships.

Although

$$Y_v' = -[(\partial C_L/\partial \alpha) + D_o']$$

Inoue and others have found that the two factors follow similar trends, and have found it expedient to combine the two. Besides, most datasets present Y_v' alone, and may or may not include resistance data.

Figure 11 shows that Jacobs' version of the Jones formula, $(\pi/2)A^2$, always overpredicts the value of Y_v', although it may come close to the destroyer data if propellers and rudders were removed (Figure 12). Inoue's more recent version runs through the data for Series 60, while it under-predicts for fine destroyers and overpredicts for full tankers (Figure 12).

Bollay's theory, expectably, well overpredicts the value of Y_v' for bare hull. From the beginning, it was obvious that ship hulls are not good approximations to flat rectangu-

lar plates. But the insight into the basic flow phenomena of vortex sheet generation has been valuable, especially in light of Saunder's photographs, showing vortex formation along a patrol craft underbody.

My conclusion is that the data should be left in the graphical form, and that data points should be added as they become available. Eventually, a function

$$Y_v' = f(A, B/L, Fn, C_B, \ldots)$$

will become evident; but for now, the graphical form with supplementary graphs for B/L and C_B dependence is clearest and most useful.

Much more basic experimental work is desirable. Such things as V form versus U form bows; systematic variations of skeg length; variations of rudder size, aspect ratio, and location relative to propeller; and LCB variation have not been examined because there are no data available. More flow studies like those of Saunders and Bertrand are necessary for basic understanding of the vortex phenomena.

Code for Figures 11 and 12

+ Jacobs Series 60, Figure 11

+ Eda Series 60, Figure 12

× Mariner

✱ Glansdorp and Pijfers tankers

⊙ MARAD tankers

△ Gerritsma, Beukelman, and Glansdorp Special Series 60

⊡ Destroyers

▽ HyA tankers

◇ Navy fleet oiler

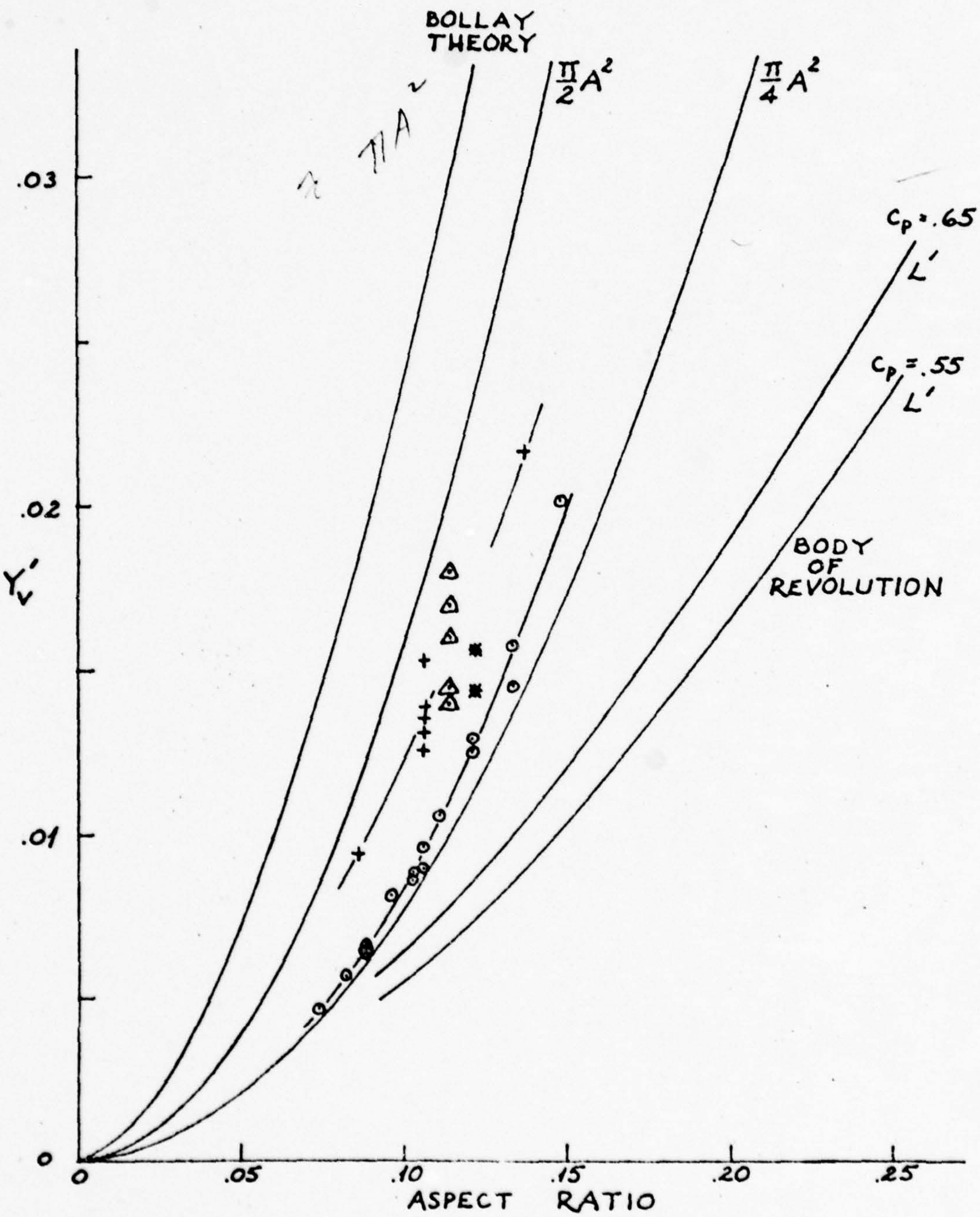

Figure 11: Y_v' versus A, Bare Hulls

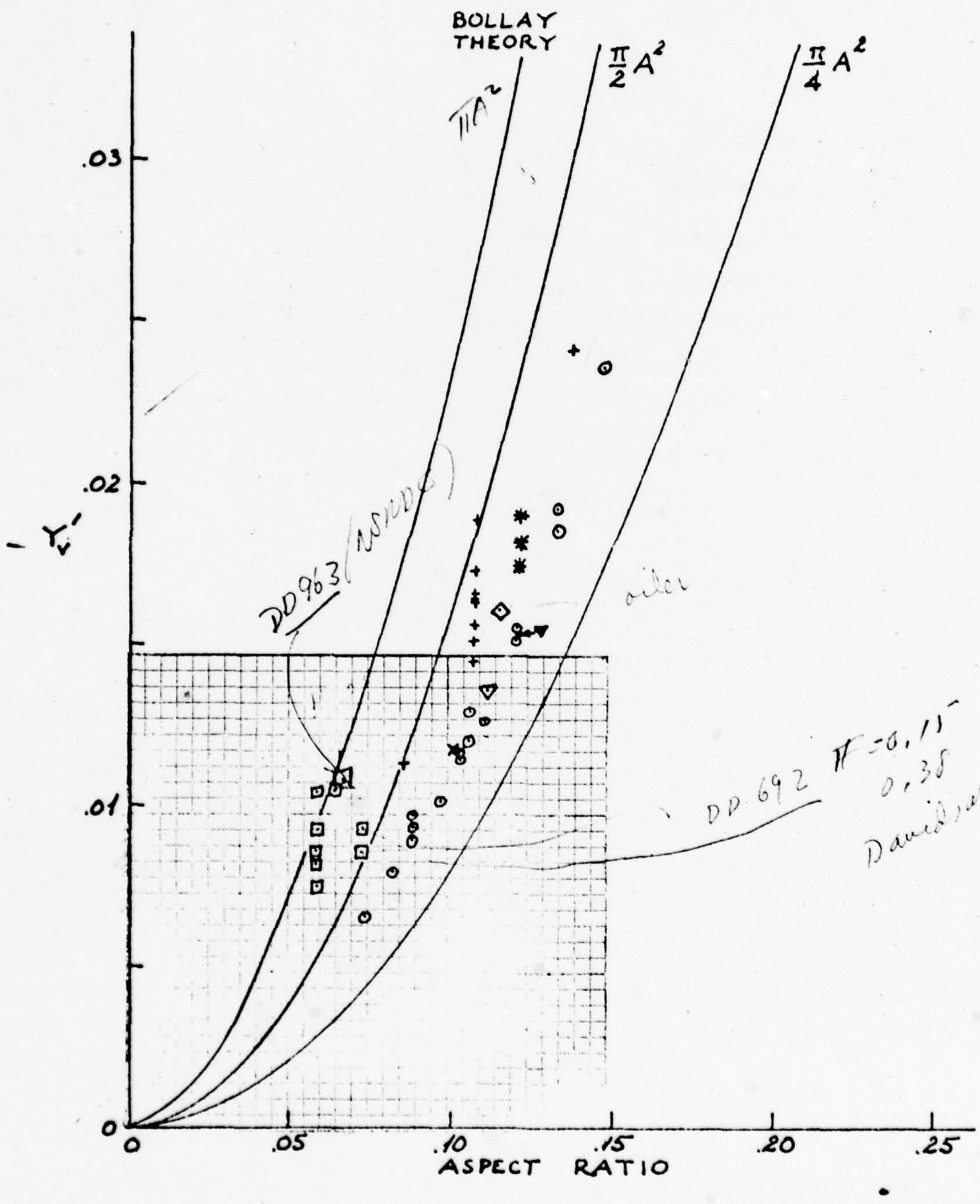

Figure 12: Y_v' versus A, with Propellers and Rudders

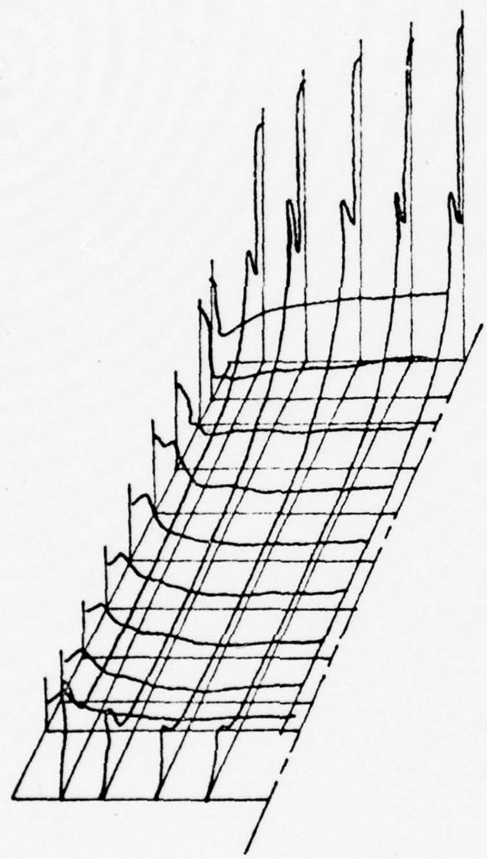

Figure 13: Pressure Distribution on Suction Side of Thin Rectangular Flat Plate, A=1, at $\alpha = 8°$ [3].

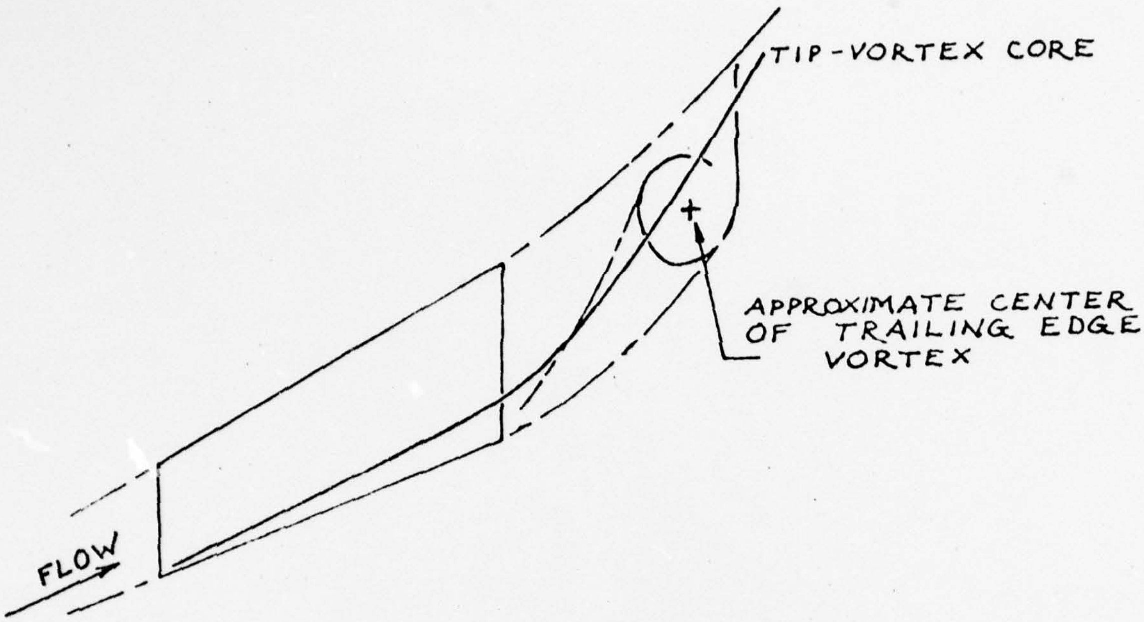

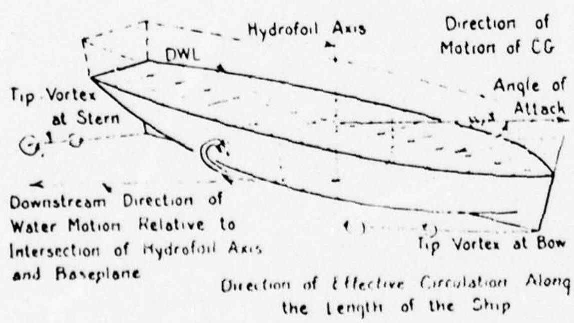

FIG. 5.B CIRCULATION IN THE TIP VORTEXES FROM A SURFACE SHIP ACTING AS A HYDROFOIL

Figure 14: Vortex Patterns for Thin Rectangular Flat Plate [3] and for Ship Hull [22] at Angle of Attack

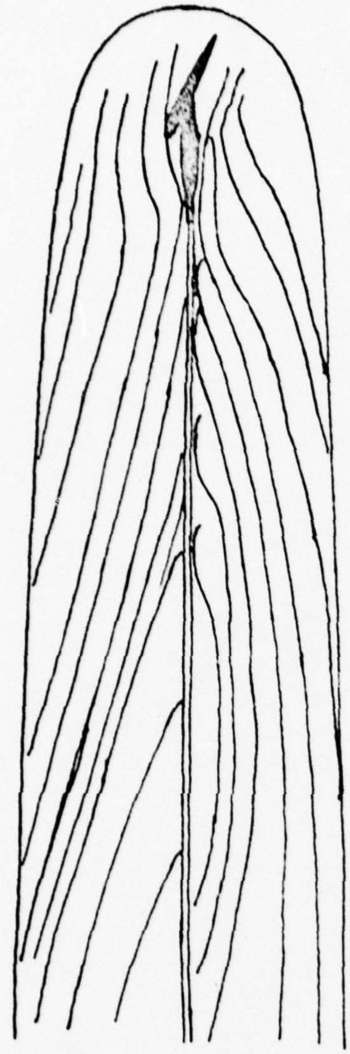

FISH-EYE VIEW OF THE CROSS FLOW UNDER AN ESCORT-SHIP MODEL WHEN TURNING

Figure 15: Excerpts from Saunders' Hydrodynamics in Ship Design Volume III [22].

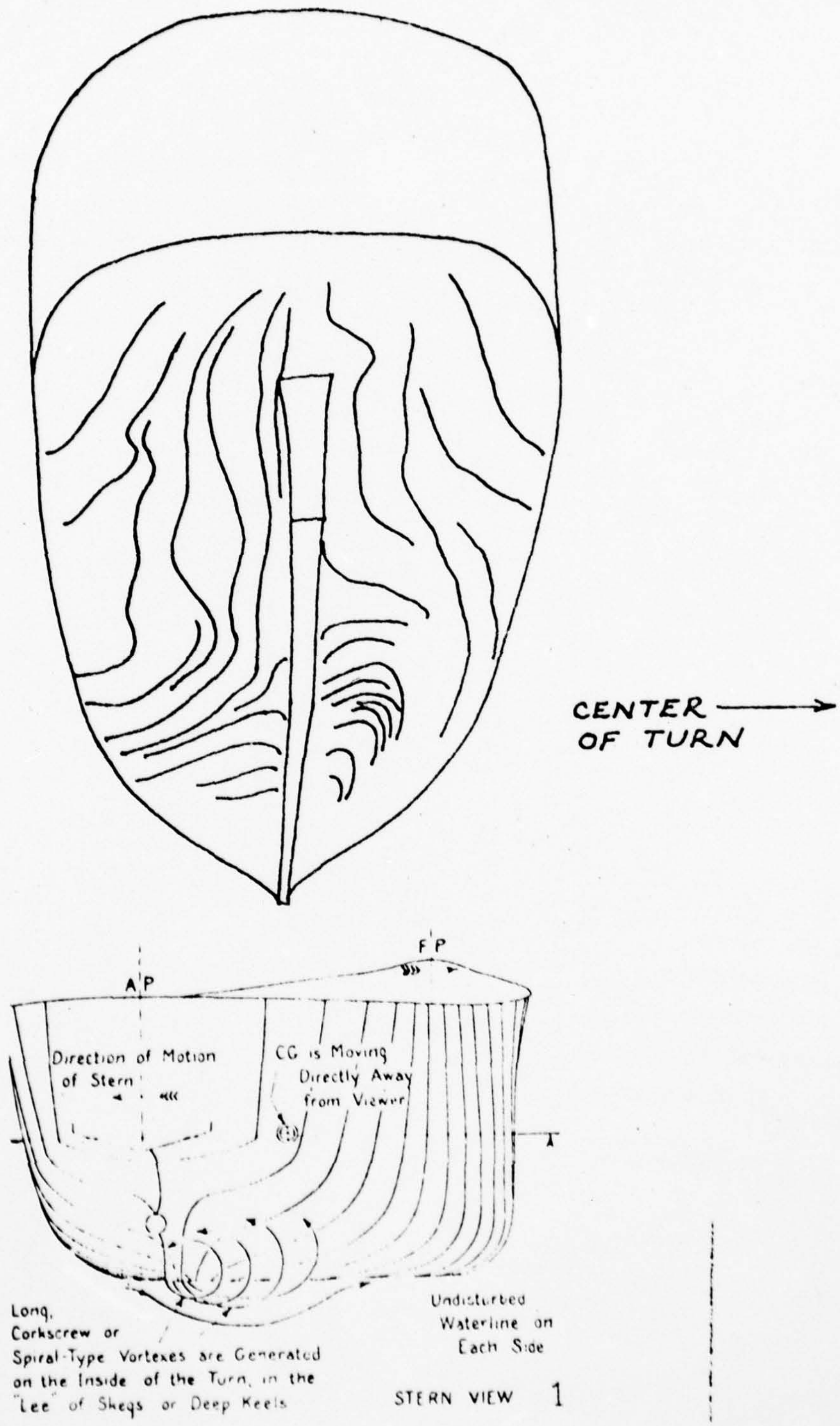

Figure 15 (continued)

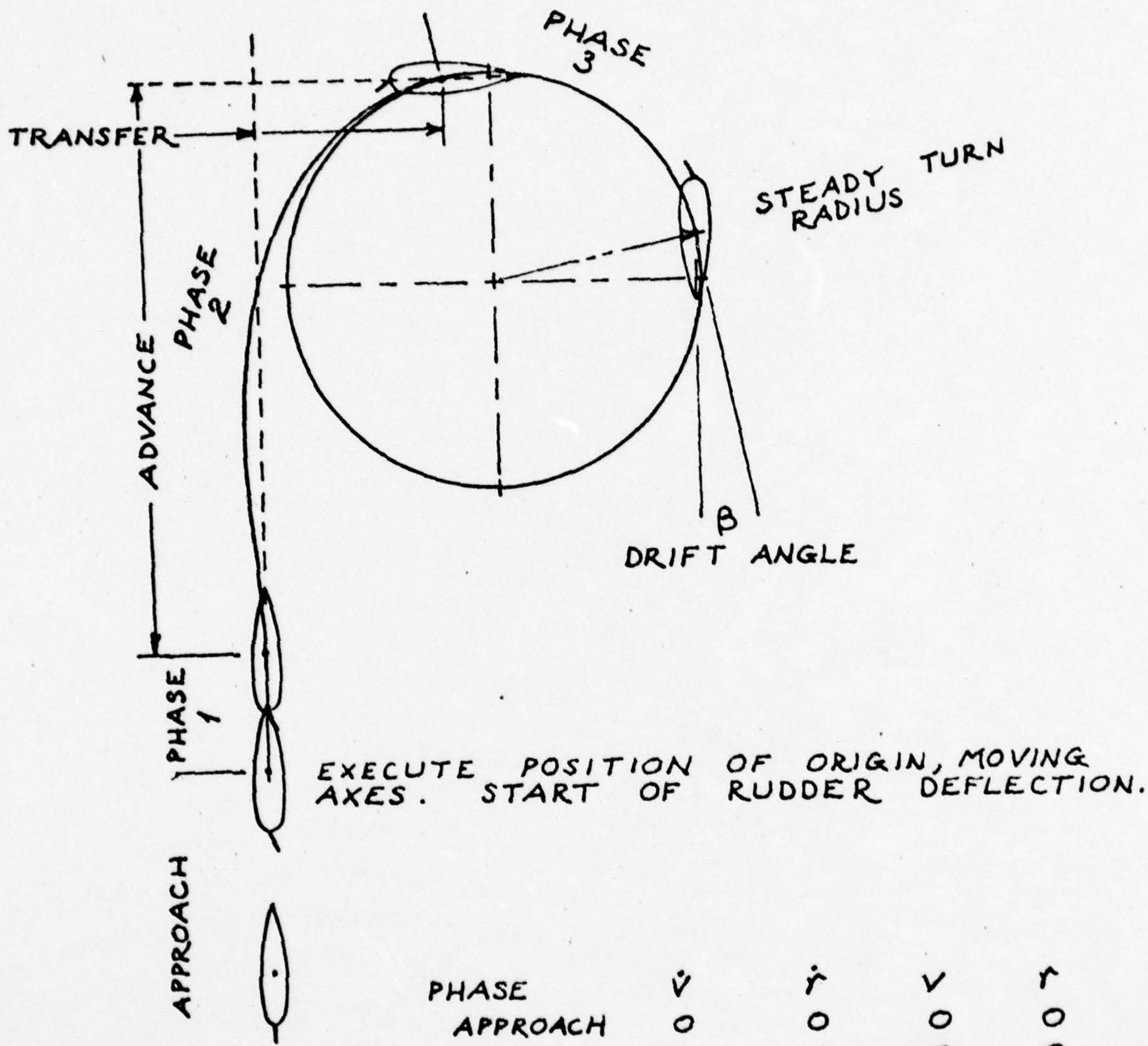

PHASE	$\dot{v}$	$\dot{r}$	v	r
APPROACH	0	0	0	0
1	$\neq 0$	$\neq 0$	0	0
2	$\neq 0$	$\neq 0$	$\neq 0$	$\neq 0$
3	0	0	$\neq 0$	$\neq 0$

Figure 16: Phase of a Turning Maneuver [9]

REFERENCES

1. Abbott, I.H. and von Doenhoff, A.E., Theory of Wing Sections, Dover, Inc., New York, 1959.

2. Abkowitz, M.A., Stability and Motion Control of Ocean Vehicles, MIT Press, Cambridge, Massachusetts, 1969.

3. Bertrand, J.E., "Experimental Investigation of Low Aspect Ratio Aerofoils," M.S. Thesis in Ocean Engineering, MIT, Cambridge, Massachusetts, January 1972.

4. Bishop, R.E.D., Burcher, R.K., Parkinson, A.G., and Price, W.G., "Oscillatory Testing for the Assessment of Ship Manoeuvrability," Tenth Naval Hydrodynamics Symposium, MIT, Cambridge, Massachusetts, July 1974.

5. Bjerregaard, E.T.D., letter to Abkowitz, M.A., from Skibsteknisk Laboratorium, Lyngby Denmark, July 1975.

6. Bollay, W., "A Theory for Rectangular Wings of Small Aspect Ratio," Journal of Aeronautical Science, Vol. 4, No. 7, May 1937.

7. Brown, S.H. and Alvestad, R., "Simulation of Maneuvering Characteristics of a Destroyer Study Ship Using a Modified Nonlinear Model," Journal of Ship Research, Vol. 19, No. 4, December 1975.

8. Chislett, M.S., letter to Abkowitz, M.A., from Hydro-Og Aerodynamisk Laboratorium (HyA), Lyngby Denmark, September 1973.

9. Comstock, J.P. (editor), Principles of Naval Architecture, The Society of Naval Architects and Marine Engineers, New York, 1967.

10. Cox, G.G. and Motter, L.E., "Prediction of Standard Maneuvering Characteristics for a Naval Auxiliary Oiler (AO177 Class)," Report SPD-624-01, Naval Ship Research and Development Center, Bethesda, Maryland, June 1975.

11. Eda, H., "Maneuvering Performance of High Speed Ships and Catamarans," Report SIT-DL-74-1626, Davidson Laboratory, Stevens Institute of Technology, Hoboken, New Jersey, January 1974.

12. Gerritsma, J., Beukelman, W., and Glansdorp, C.C., "The Effects of Beam on the Hydrodynamic Characteristics of Ship Hulls," Tenth Naval Hydrodynamics Symposium, MIT, Cambridge, Massachusetts, July 1974.

13. Gertler, M. and Kohl, R.E., "Resistance, Propulsion, and Maneuverability Characteristics of MARAD Systematic Series for Large Full-Form Merchant Ships," Report 7370-1, Hydronautics, Inc., Laurel, Maryland, November 1974.

14. Glansdorp, Ir. C.C., and Pijfers, J.G.L., "The Effect of Design Modifications on the Natural Course Stability of Full Tanker Models," Report 335, Laboratorium Voor Scheepsbouwkunde, Technische Hogeschool Delft, The Netherlands, November 1971.

15. Hoak, D.E. (project engineer), USAF Stability and Control DATCOM, Flight Control Division, Air Force Flight Dynamics Laboratory, Wright-Patterson Air Force Base, Ohio, October 1960 (revised January 1976).

16. Inoue, S., "The Determination of Transverse Hydrodynamic Nonlinear Forces by Means of Steady Turning," Eleventh International Towing Tank Conference Proceedings, Tokyo Japan, October 1966.

17. Jacobs, W.R., "Method of Predicting Course Stability and Turning Qualities of Ships," Report 945, Davidson Laboratory, Stevens Institute of Technology, Hoboken, New Jersey, March 1963.

18. Jacobs, W.R., "Estimation of Stability Derivatives and Indices of Various Ship Forms, and Comparison with Experimental Results," Report 1035, Davidson Laboratory, September 1964.

19. Jones, R.T., "Properties of Low-Aspect-Ratio Pointed Wings at Speeds Below and Above the Speed of Sound," Report 835, NACA.

20. Landweber, L. and Johnson, J.L., "Prediction of Dynamic Stability Derivatives of an Elongated Body of Revolution," Report C-359 (recently declassified), David Taylor Model Basin, Washington, D.C., May 1951.

21. Munk, M.M., Aerodynamic Theory of Airships, W.F. Durand, Editor, Julius Springer, 1934.

22. Saunders, H.E., Hydrodynamics in Ship Design, Vol. III, The Society of Naval Architects and Marine Engineers, New York, 1965.

23. Strom-Tejsen, J., "A Digital Computer Technique for Prediction of Standard Maneuvers of Surface Ships," Report 2130, David Taylor Model Basin, Washington, D.C. December 1965.

24. Surber, W.G. Jr., "Turning and Maneuvering Tests of Model 4945 Representing the U.S. Coast Guard 350-foot High Endurance Cutter with the "V" Form Bow," Report 1835, David Taylor Model Basin, Washington, D.C., April 1964.

25. Todd, F.H., "Series 60 Methodical Experiments with Models of Single-Screw Merchant Ships," Report 1712, David Taylor Model Basin, Washington, D.C., July 1963.

APPENDIX I

Some Established Characteristics of Hydrodynamic Derivatives

1) X_u represents the slope of the curve of the X force plotted against Δu. Direction of X force is opposite to direction of drag or resistance force. X_u will be negative as long as the net drag increases with speed. For displacement ships, X_u will be large. For planing or other non-displacement ships, at the point of planing or lift-off the drag can decrease with an increase in speed, making X_u a positive quantity, briefly. X as a force represents the imbalance between drag or resistance force and force provided by propeller thrust. At equilibrium speed u_o, $X = 0$.

2) $X_{\dot{u}}\dot{u}$ represents the force that the body experiences in the x-direction as a result of acceleration in the x-direction. The inertial reaction force of the fluid against the acceleration that the body causes is in the direction opposite to the acceleration of the body. $X_{\dot{u}}$ is negative and is 5% to 10% of the mass for normal ship types.

3) $Y_{\dot{v}}\dot{v}$ represents the linear approximation of the Y force resulting from acceleration in the y-direction. The origin

of the force is similar to that for $X_{\dot{u}}\dot{u}$. $Y_{\dot{v}}$ for both bow and stern is strongly negative, the magnitude being close to that of the mass for normal ship types.

4) $N_{\dot{r}}\dot{r}$ represents the linear approximation of the moment resulting from angular acceleration about the origin of the axis system fixed in the body. A positive $\dot{r}$ produces a local $\dot{v} = \dot{r}d_b$ at each point P(b) forward of the origin and a local $\dot{v} = -\dot{r}d_s$ at each point P(s) aft of the origin. The inertial reaction force of the fluid against the acceleration is a hydrodynamic force in the direction opposite to the acceleration. The moments caused by the forces add to produce a significant negative value for positive $\dot{r}$.

5) $Y_{\dot{r}}\dot{r}$ results from the imbalance of the forces which cause $N_{\dot{r}}\dot{r}$. But for $Y_{\dot{r}}\dot{r}$, the forces on the bow are in the direction opposite to the direction of the forces on the stern. Hence, $Y_{\dot{r}}\dot{r}$ may be (+), (-), or in rare cases, zero. The magnitude of $Y_{\dot{r}}$ will be small. If the bow predominates, having greater pressure distribution, $Y_{\dot{r}}$ will be negative.

6) $N_{\dot{v}}\dot{v}$ arises from the same hydrodynamic inertial reaction that causes $Y_{\dot{v}}\dot{v}$. But since the bow and stern forces are in the same direction, $N_{\dot{v}}\dot{v}$ will result from an imbalance. Hence

the magnitude of $N_{\dot{v}}$ may be (+), (-), or zero. The magnitude of $N_{\dot{v}}$ will be small. If the bow predominates, $N_{\dot{v}}$ will be negative.

7) $Y_v v$ results from the steady-state lift that arises from the angle of attack of the body as it moves ahead at velocity u_o and to the side at velocity v. A positive v causes forces in the negative y-direction on all sections along the length of the body. These forces add to give a significant negative value to Y_v.

8) $N_v v$ arises from the same hydrodynamic lift forces that cause $Y_v v$. But as with $N_{\dot{v}}\dot{v}$, the imbalance of bow and stern forces causes N_v to be (+), (-), or zero, and to have small magnitude. If the bow forces predominate, N_v will be negative.

9) $Y_r r$ arises from the lift generated as the angle of attack increases as the body moves ahead at velocity u_o. A positive r causes negative Y forces on the bow and positive Y forces on the stern. Y_r represents the imbalance of these forces, hence it will be small. If bow forces predominate, Y_r will be negative.

10) $N_r r$ has the same origin as $Y_r r$, but now the bow and stern forces add to make N_r a significant negative value.

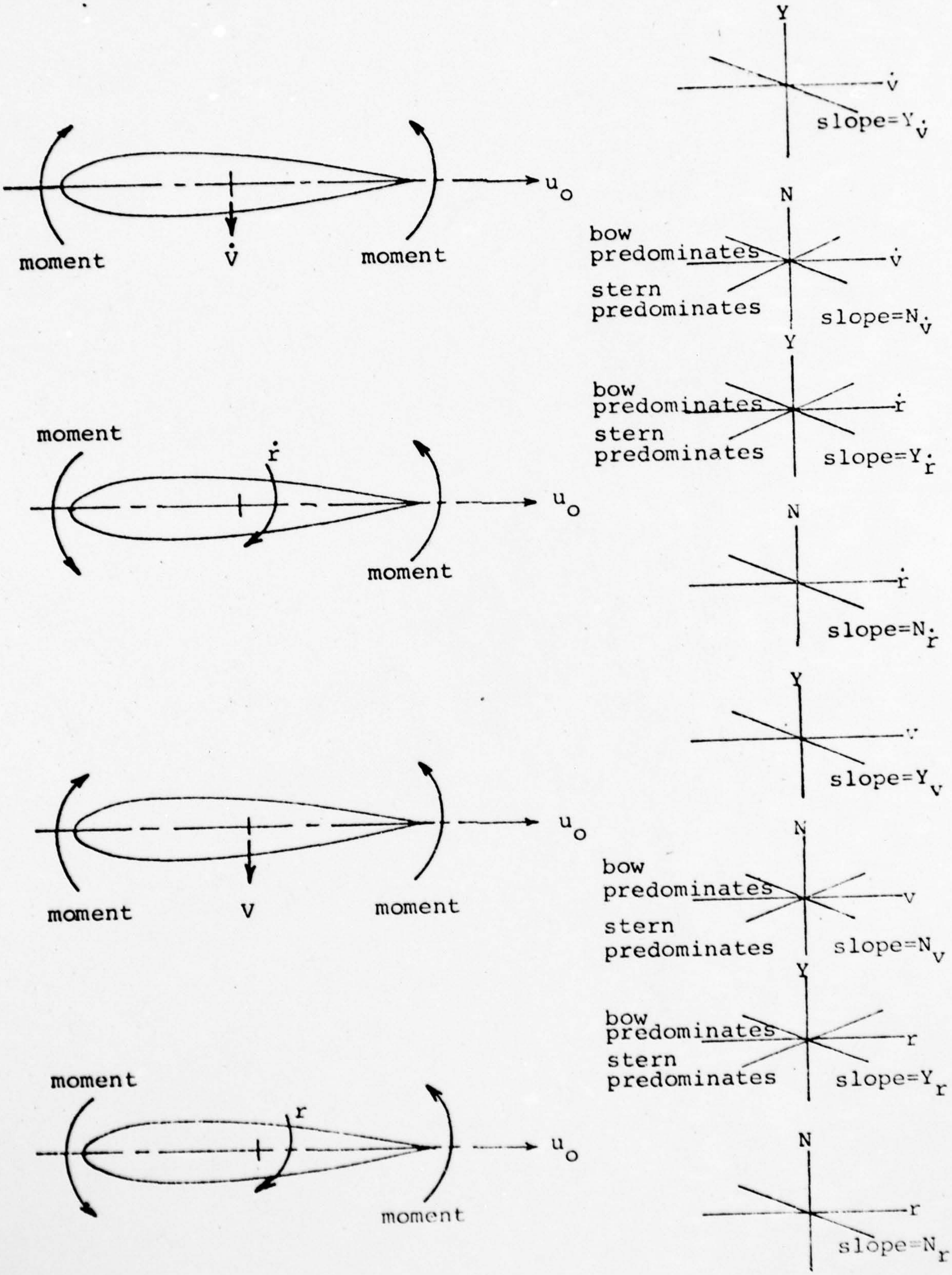
Y
v̇
slope=$Y_{\dot{v}}$
u_o
moment
v̇
moment
N
bow
predominates
v̇
stern
predominates
slope=$N_{\dot{v}}$
Y
bow
predominates
ṙ
stern
predominates
slope=$Y_{\dot{r}}$
moment
ṙ
u_o
moment
N
ṙ
slope=$N_{\dot{r}}$
Y
v
slope=Y_v
u_o
moment
v
moment
N
bow
predominates
v
stern
predominates
slope=N_v
Y
bow
predominates
r
stern
predominates
slope=Y_r
moment
r
u_o
moment
N
r
slope=N_r

$Y_{\dot{v}}$	bow and stern effects add, have (-)
$N_{\dot{v}}$	bow and stern effects are opposite, have (+), (-), or 0
$Y_{\dot{r}}$	bow and stern effects are opposite, have (+), (-), or 0
$N_{\dot{r}}$	bow and stern effects add, have (-)
Y_v	bow and stern effects add, have (-)
N_v	bow and stern effects are opposite, have (+), (-), or 0
Y_r	bow and stern effects are opposite, have (+), (-), or 0
N_r	bow and stern effects add, have (-)

APPENDIX II

Munk Moment versus Actual Moment [Empirical] for Submarines

In non-viscous flow, unstable moment for forward motion is proportional to $(k_2 - k_1)$ where k_2 and k_1 are coefficients of added mass in lateral and longitudinal directions.

Munk Moment = moment of instability = $(k_2 - k_1)\nabla\rho(V^2/2)\sin 2\alpha$

Empirical formula for submarines (roughly, an ellipsoid of revolution) [20],

$$M_w' = 0.87(k_2 - k_1)m' = -N_v'$$

$$= M_w/\tfrac{1}{2}\rho L^3 u$$

$$m' = m/\tfrac{1}{2}\rho L^3 = 2\nabla/L^3 \quad ; \quad \nabla = \text{displaced volume}$$

For ellipsoid of revolution, $\nabla = \frac{4}{3}\pi b^2 a$; $2a = L$, $2b = H$

Therefore,

$$M_w' = 0.87(k_2 - k_1)\frac{8}{3}\frac{\pi b^2 a}{(2a)^3} = 0.87(k_2 - k_1)\frac{\pi b^2}{3a^2}$$

AD-A071 286 MASSACHUSETTS INST OF TECH CAMBRIDGE DEPT OF OCEAN E--ETC F/G 13/10
ANALYSIS OF THE LATERAL FORCE COEFFICIENT FOR SHIP MANEUVERING --ETC(U)
JUN 76 R STANLEY N00014-75-C-1006
UNCLASSIFIED NL

2 OF 2
AD
A071286

END
DATE
FILMED
8-79
DDC

In this form, $(k_2 - k_1)\frac{\pi b^2}{3a^2}$ = Munk Moment (non-dimensional derivative w.r.t. vertical velocity)

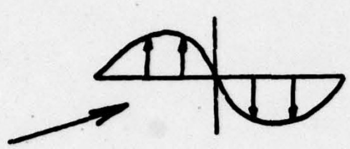

Pressure forces in potential, non-viscous flow, due to 2 stagnation points.

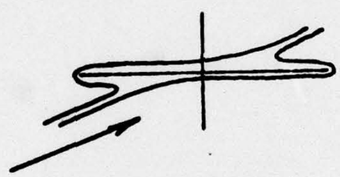

In potential flow with circulation, the aft stagnation point moves to the tail to satisfy the Kutta condition:

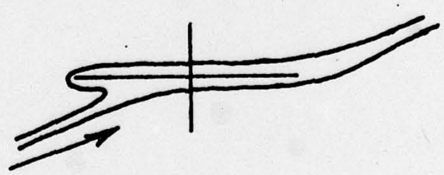

This is brought about by circulation flow about the airfoil:

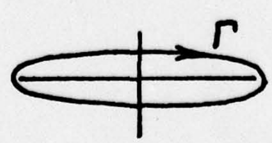

which, when combined with the incoming flow, creates lift, the pressure distribution for which is, typically:

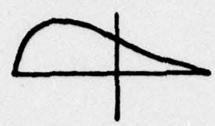

The net effect is to redistribute the forces which cause the moment of instability:

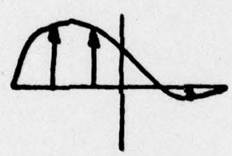

and, in the submarine case, to reduce the moment by 13%. Hence,

$$\text{(Lift x moment arm)} = \text{(Munk Moment)} - \text{(Actual Moment)}$$
$$= \text{(Munk Moment)} - .87\text{(Munk Moment)}$$
$$= 0.13\text{(Munk Moment)}$$

$Z_w' = -0.234m'^{0.79} - D'$

$L_w' = Z_w' + D' = -0.234m'^{0.79}$

$L_w = L_w'\frac{1}{2}\rho L^2u$

$M_w = M_w'\frac{1}{2}\rho L^3u$

Thus, Munk Moment = $(k_2 - k_1)\frac{\pi}{3}(\frac{b}{a})^2 \frac{1}{2}\rho\, 8a^3u$

$$\text{Lift} = -0.234[\frac{\pi}{3}(\frac{b}{a})^2]^{0.79} \times \frac{1}{2}\rho\, 4a^2u$$

$$\text{Moment arm} = \frac{0.13(k_2 - k_1)(\pi/3)(b/a)^2(1/2\,\rho\, 8a^3u)}{0.234[(\pi/3)(b/a)^2]^{0.79}(1/2\,\rho\, 4a^2u)}$$

$$= \frac{(k_2 - k_1)(b/a)^2 a}{(b/a)^{1.58}} \times 1.1219$$

$$= (k_2-k_1)(b/a)^{.42} \times 1.122a$$

$$= (k_2-k_1)(b/a)^{.42} 0.561L$$

b/a	1/4	1/5	1/6	1/7	1.8
k_2	.862	.895	.917	.933	.945
k_1	.082	.060	.046	.035	.029
Moment arm	.24445L	.23828L	.23023L	.22248L	.21457L
Moment arm -L/4	-.00555L	-.01172L	-.01977L	-.02752L	-.03543L